A STUDY OF A MULTITUDE OF PROPPANTS FOR FRACTURE CONDUCTIVITY OF UNCONVENTIONAL RESOURCES

A Thesis

by

JAMES NICOLAS FERNANDEZ

Submitted to the Office of Graduate and Professional Studies of
Texas A&M University
in partial fulfillment of the requirements for the degree of

MASTER OF SCIENCE

Chair of Committee,	Ding Zhu
Co-Chair of Committee,	A. Daniel Hill
Committee Member,	Debjyoti Banerjee
Head of Department,	Jeff Spath

May 2019

Major Subject: Petroleum Engineering

ABSTRACT

Onshore Oil and Gas production in the United States today primarily consists of exploiting unconventional shale reservoirs. Due to the low permeability of this type of formation, a stimulation method is required. A very common and effective method is hydraulic fracturing. The costs of hydraulic fracturing is highly variable and is dependent on many criteria, such as the cost of pumping proppant. Proppant in hydraulic fracturing maintains the fracture network open once the closure stress of the reservoir is applied, allowing for the flow of fluids to the wellbore. The mass quantity of proppant is dependent of the size of the hydraulic fracturing job. The cost of a fracture treatment can fluctuate due to the location, quantity, and quality of the proppant. The objective of this study is to find alternative proppants that can provide technical merit and economic benefits.

A multitude of proppants were tested for this study including local and premium sands, as well as taconite tailings, which is a low-grade iron ore. These proppants were tested in a variety of mesh sizes. The fracture conductivity and the strength of each proppant were compared under idealized conditions, utilizing the standard API conductivity test cell.

Fracture conductivity is the ability of a proppant pack to transport fracture fluid to through the fracture. Thus, a measurement of this value can provide insight into the effectiveness of the stimulation. The testing of fracture conductivity regarding all proppants will be adhered to by the API RP 61 procedure. This procedure is the recommended practice for evaluating short term proppant pack conductivity and has been

put in place by the American Petroleum Institute. Proppant is the solids used in hydraulic fracturing that maintains the fracture open once the pumping is stopped and the reservoir closure stress is applied to the fracture. Proppant can be natural sands or man mad materials, such as ceramics.

As per the recommendation of API RP 61, a series of closure stresses is utilized ranging from 1000 psi – 6000 psi, in 1000 psi intervals, in order to test the fracture conductivity. To obtain results that relate to the strength of an individual proppant, a sieve analysis is conducted before and after a fracture conductivity test is completed. The sieve analysis provides a size distribution of the proppant ranging from 20 mesh-170 mesh. Thus, once the proppant has been exposed to very high closure stress, it experiences crushing of some sort. The size distribution of the proppant after crushing is then be compared to the initial distribution.

As can be expected, all proppants display a higher conductivity when a larger proppant mesh size is used. The strength of the proppant, relating to the Young's modulus of the material, as well as the shape, help to further validate the results of the testing. Overall, conventional sand provided better and more consistent conductivity. The conductivity of the taconite shows a wide range of results that is highly dependent on the purity of the proppant sample.

DEDICATION

I would like to thank my family and friends who have always been a motivating factor in my pursuit of higher education. Your unwavered support means the world to me.

ACKNOWLEDGEMENTS

I would like to thank my advisor and committee chair, Dr. Zhu, for the opportunity to pursue my graduate degree while being fully funded. Dr. Zhu has been a mentor, providing advice regarding research, as well as future career opportunities. I would not have been able to obtain my degree from such a wonderful university without your guidance. As well, I would like to thank my co-chair, Dr. Hill. His open-door policy was very much appreciated and made me feel welcome to have candid discussion with him. Thank you both very much. Lastly, I would like to thank Dr. Banerjee from the Department of Mechanical Engineering for being my out of department committee member.

I would also like to thank Fabian Carrascal and Jimmy Jin who have helped me in all facets of conducting experiments. Your patience, advice, and help were all greatly appreciated.

Lastly, I would like to Texas A&M University. Pursuing my graduate degree here has been one of the best decisions I've ever made. I have met wonderful people and created friendships that will last a lifetime. Thank you for welcoming me into the Aggie family with open arms. Gig 'Em, always!

CONTRIBUTORS AND FUNDING SOURCES

Contributors

This study was conducted under the committee supervision of Dr. Ding Zhu and Dr. Daniel Hill of the Harold Vance Department of Petroleum Engineering, as well as Dr. Debjyoti Banerjee of the Department of Mechanical Engineering.

Technical assistance was provided by Fabian Carrascal and Jimmy Jin of the Harold Vance Department of Petroleum Engineering.

All other work conducted for this thesis was completed by the student independently.

Funding Sources

Graduate study was supported by a fellowship from Texas A&M University and a Research Assistantship for the study of fracture conductivity was provided by Marathon Oil.

NOMENCLATURE

q	Flow rate
A	Cross-sectional area
w_f	Fracture width (thickness)
h_f	Fracture height (width)
k_f	Fracture permeability
L	Length over which pressure drop occurs
M	Molecular weight of fluid
p1	Upstream pressure
p2	Downstream pressure
R	Universal Gas Constant
T	Temperature
v	Fluid velocity
Z	Gas compressibility factor
ρ	Density of fluid
μ	Viscosity of fluid
Δp	Differential pressure across proppant pack
C_f	Fracture Conductivity

TABLE OF CONTENTS

Page

LIST OF FIGURES

Page

LIST OF TABLES

Page

1. INTRODUCTION AND LITERATURE REVIEW

1.1 Background

The production of oil and gas over many decades has led to the depletion of conventional reservoirs, which are ones with a relatively high permeability and porosity. Because of this, the source rocks that provide conventional reservoirs with the hydrocarbons, are now being explored. The source rocks are primarily a shale rock and is defined as an unconventional reservoir because they have very low permeability and porosity. These unconventional reservoirs require extensive stimulation treatments, known as hydraulic fracturing.

Hydraulic fracturing is the process of pumping mass quantities of highly engineered fluid and proppant into the formation to create fractures that allow natural resources to eventually reach the wellbore and be produced. This process is necessary, being that shale formations have extremely low permeability and would not allow for production to occur naturally. Initially, frac fluid is pumped into the formation to initiate cracks. Once the fluid pressure decreases, this is indicative of a substantial pathway having been created. Naturally the ground will close together due to the overburden pressure of the formation, once the pumping pressure is stopped.

In order to maintain the pathways that have been opened, proppant is then pumped with the fluid mixture. The overburden pressure of the ground will again act on the pathways, however the proppant that is in place will preserve the fractures and allow for flow to occur.

1.2 Literature Review

1.2.1 Hydraulic Fracturing

Hydraulic fracturing is a stimulation method that has been in use since 1949 when Stanolind Oil began using the technology (Clark, 1949). Over this period of nearly 70 years, many things have changed regarding hydraulic fracturing, however, the principles behind the stimulation have remained unchanged. During the initial experimental stage, it was necessary to find a fluid that could act with a high viscosity in order to fracture the rock and not simply seep into the formation and then become less viscous, allowing for flowback of hydrocarbons. Fluids that were used included Napalm that was added to Gasoline, Kerosene, and other refined products. As well, injection rates of the fracturing fluid were typically 3 bbl/min at pumping pressures commonly around 1,500 psi.

As hydraulic fracturing advanced, closer investigation was given to the type of fracturing fluid being used, as well as the amount of proppant applied downhole. A change from oil-based fluid to water-based fluid was made during the 1970's, so much so that 75-80% of all hydraulic fracturing treatments that employed propping agents, utilized this water-based fluid (Coulter 1976). During this time, advancements in crosslinked gels that were added to the water-based fluids, were found to create an extremely high viscous fluid which allowed proppant to travel a much greater distance into the fracture, as well as provide a better distribution of said proppant. In addition, it was found that pumping at a higher rate and with a greater volume of proppant resulted

in a more effective stimulation. Thus, the flow rates were increased to anywhere from 25-60 bpm and commonly used 500,000 pounds of proppant.

Hydraulic fracturing procedures were primarily used in tight gas reservoirs during this time. As the first decade of the 2000's ended, interest in the oil and gas industry shifted to the exploitation of shale, which is the source rock to a reservoir. Shale poses difficulty to produce hydrocarbons because of the extremely low permeability of the rock. Thus, hydraulic fracturing is the best practice in order to produce from such a rock. Horizontal wells were proven to be the most efficient method of drilling and producing from the shale reservoirs and multi well locations became the norm in order to reduce the environmental impact and drilling costs. The key to success in shale resources is maximizing reservoir contact (Auzerais, 2014). Technological advancements continued to refine hydraulic fracturing and the process is now very well understood. Multistage stimulation jobs are commonly utilizing up to 40 stages per well. This is in addition to the increased fluid flowrate in excess of 100 bpm and a quantity of up to 2.5 million pounds of proppant that is sent downhole.

A significant change made to hydraulic fracturing processes was the transition from crosslinked gel fracturing fluid to slickwater, which is merely water that has been slickened with a friction reducer or gel, in order to reduce frictional forces within the wellbore. There are many pros and cons that have resulted from this change. The use of slickwater reduces the amount of gel damage within the fracture by up to a factor of four, reducing the chemical package necessary. A slickwater stimulation will also provide a better fracture network due to the low viscosity of the fluid and higher

injection rates. The cost benefit of slickwater versus crosslinked gel has many variables at play. The location of a water source plays an important role since a very large volume of water is needed. As well, due to the highly viscous nature of slickwater, proppant placement is the prime concern. Most of the low viscosity fluids being used in slickwater fracturing have little ability to suspend and/or transport proppant (Palisch et. al., 2008). To overcome this issue, very low proppant concentrations are used, on the order of 3 lb/gal, in addition to a very high flow rate, as previously mentioned. With this issue, conductivity of the fracture network becomes a concern.

1.2.2 Fracture Conductivity

Fracture conductivity has received great interest since the inception of hydraulic fracturing because it is the measure of the quality of stimulation. Fracture conductivity is the product of the proppant pack permeability multiplied by the fracture width, as defined by C.E. Cooke (1973). Cooke was a leader in fracture conductivity research beginning in the 1970's. Fracture conductivity is representative of the ability for fluids to flow through a proppant pack. Variables that can have an altering effect on fracture conductivity are the type, size, shape, and quantity of the proppant, all of which can change the ability for a fluid to flow through the fracture. Countless combinations of these variables have been utilized to find the most effective treatment.

1.2.3 Proppant

The understanding of the function and the behavior of proppant is of the upmost importance regarding hydraulic fracturing because it is the driving force behind fracture conductivity. As previously mentioned, fracture conductivity is the product of the

proppant pack permeability and the fracture width. What maintains the fracture width and in a larger perspective, the fracture network, is indeed the proppant. Initial use of a propping agent allowed for an increased production, however, rapid decline in the stimulation effect led to studies of proppants that continue to this day (Weaver et. al., 2005). Throughout the nearly 70 years of hydraulic fracturing, sand has been the primary proppant used. Although studies have been conducted to test the feasibility of using other materials as propping agents, they have not proven to be more effective as a standalone proppant than standard quartz. The proppant used in hydraulic fracturing treatments endure extremely high closure stresses. If the materials crush, it follows that the conductivity of the proppant-packed fracture will be diminished, reducing conductivity and well production (Weaver et. al, 2005). In order to combat this, studies have been conducted regarding all aspects of the proppant including, but not limited to the size distribution, the sphericity, the material properties, and the proppant placement.

Propping material for hydraulic fracturing use comes in a variety of sizes and shapes. This size is defined by a sieve analysis, which is a mesh interface that allows proppant to pass through. A proppant size is defined by a percentage of proppant that passes through a larger mesh and is upheld by a smaller one. A 20/40 mesh proppant follows such a rule that 90% of the proppant should pass through the 40-mesh sieve and be retained by the 70-mesh sieve. The oil and gas industry will commonly use proppant as large as 8 mesh (2.38 mm) and as small as 140 mesh (.105 mm) (Kong, 2014).

Many factors play a role in determining the appropriately sized proppant for an individual fracturing job. As the concept that fracture conductivity is directly related to

flowrate and thus production, it might be expected that the largest possible mesh size be used. While a larger proppant will result in a larger proppant pack permeability, there are definitive drawbacks to this concept. Being that a larger proppant will have a larger density, premature settling of the proppant will become an issue. As well, the inability for the proppant to reach the end of the fracture also becomes an issue. Dimensionless fracture conductivity, defined as the fracture conductivity divided by the product of the reservoir permeability and the fracture half length, provides a means of optimizing the amount of conductivity in a fracture for varying permeability and fracture length. As the size of the proppant increases, a maximum productivity index will be reached and then begin to decline. Low permeability reservoirs, such as shale, benefit from proppant with smaller diameters because it can assist in creating a large effective fracture area, while still enhancing the permeability of the reservoir, thus allowing for a maximum well productivity to be obtained (Kong et. al, 2015). Multi-sized proppant combinations are now utilized because it allows for smaller proppant to first reach the fracture tip and then for larger proppant to maintain the fracture open near the wellbore.

The proppant pack permeability is a direct result of the size of proppant used. Larger sized proppant will lead to a more permeable proppant pack; however, a larger mesh proppant will undergo more changes than its smaller counterpart. A primary change that the proppant will experience is crushing. Standard crush test indicate that large-mesh proppants experience much higher crush under identical closure stress than smaller particles of the same materials (Palisch et. al, 2010). A proppant manufacturer conducted a study in which it found that a 20/40 mesh ceramic proppant reported

crushing of 5% at 7500 psi, meanwhile the larger sized 16/20 mesh proppant experienced crushing on the order of 20%, roughly four times more. (CARBO Ceramics, 2014).

Inherently, this lends to the idea that a larger proppant is weaker than its smaller counterpart. This however, is far from the truth. Single-pellet crush tests have revealed that larger particles require more pounds of force in order to induce failure, indicating that they are indeed stronger than comparative smaller particles (Palisch et. al, 2010). Since stimulation jobs are conducted on a mass basis, i.e. 1 million pounds per stage, it would require more small particles to maintain the same mass as that of large particles. Thus, the distribution of the closure stress is spread over a larger number of individual particles, reducing the applied force that a single grain experiences, in turn reducing the crushing of the proppant.

Once a proppant has undergone crushing, the small fragments are referred to as fines. Fines migration, or the movement of the crushed proppant, becomes an issue because it can lead to settling of the proppant or reduce the permeability of the proppant pack by filling in pore space. A lower strength proppant will result in greater crushing and thus, will experience a greater proportion of smaller fragments (Schubarth and Milton-Taylor, 2004). Fines migration decreases the fracture conductivity, having a negative effect on production because it provides an obstruction to flow. A study by Coulter et. Al. (1972) found that a crushing resulting in fines of 5% reduces proppant conductivity by 50%.

The use of proppant during the hydraulic fracturing process is to maintain a pathway that will allow for the flow of hydrocarbons. As previously mentioned, hydraulic fracturing is the process of pumping a slurry mixture at very high rates into a low permeability reservoir in order to overcome the closure stress and create a fracture. Once the pumping of the slurry has stopped, the natural closure stress of the reservoir will be reapplied to the contacting surface of the proppant where it can become embedded into the surface of the hydraulic fracture, reducing the fracture aperture (Alramahi and Sundberg, 2012). As well, proppant embedment leads to shale flakes and fine migration, negatively affecting the permeability of the proppant pack. Proppant embedment is strongly correlated to the Young's Modulus of the proppant used, which dictates its elastic stiffness. A study by Alramahi and Sundberg (2012) shows that embedment increases with the decrease in Young's Modulus. Mineralogical properties of both the proppant and the fracture surface play an important role in whether substantial embedment will take place. Proppant embedment is also more prevalent in liquid permeates than gaseous permeates, because of fracture softening (Ghanizadeh et.al, 2016). Figure 1.1 shows the effects of proppant embedment on fracture conductivity.

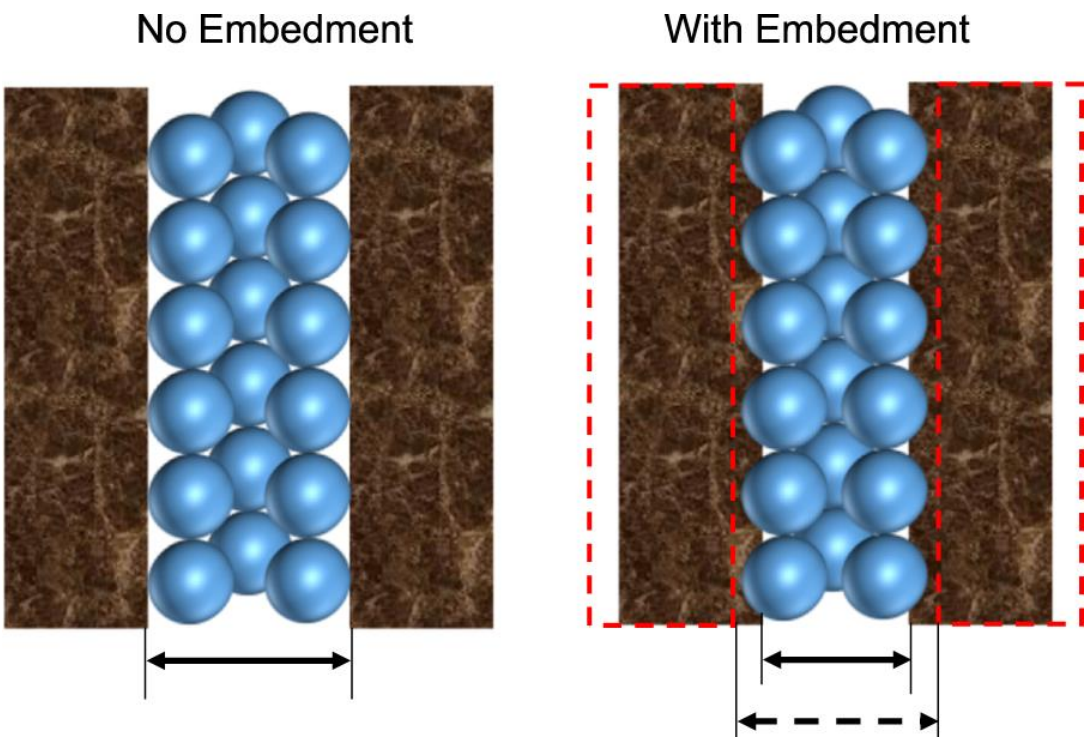

Figure 1.1 Effects of proppant embedment

Proppant geometry is a criterion that plays a large role in the success of hydraulic fracturing. In order to maintain conductivity of the fracture, the permeability of the proppant pack must be able to be retained. The shape and sphericity of a given proppant influences said conductivity when the closure stress of the reservoir is applied. Sphericity is defined as the deviation of the shape of a particle from being a perfect sphere. If a cohesion of particles takes place when the closure stress is applied, porosity of the proppant pack will be highly reduced. A more spherically shaped proppant will provide a higher permeability because of the particles contact with one another, while an angular proppant pack will fit together more tightly, resulting in a reduction of the permeability of the proppant pack. However, the angularity of a proppant, has a positive

effect on the stability of the pack and would allow for the fracture to remain open for a much greater time period (Mollanouri-Shamsi et. al., 2018).

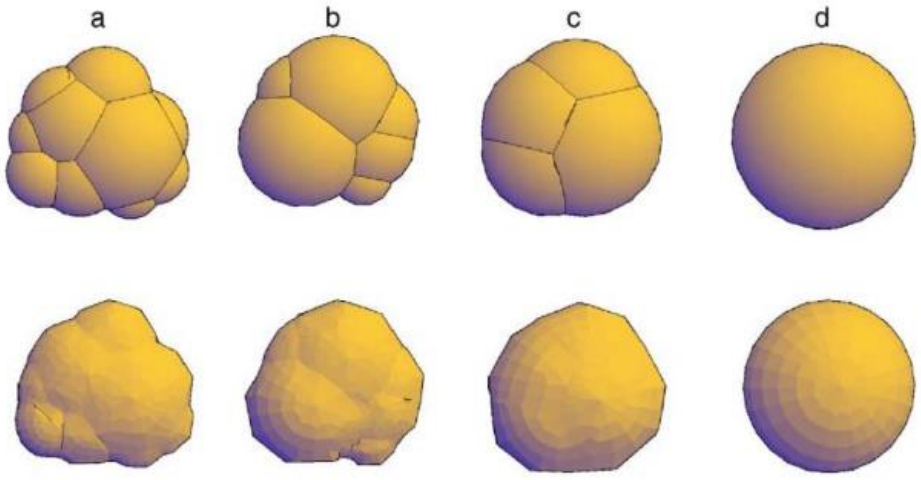

Figure 1—Four different types of proppant shape, (a) high angular proppant, (b) medium angular proppant, (c) rounded proppant, and (d) spherical proppant. (Source: Mollanouri Shamsi and Mirghasemi, 2012)

Figure 1.2 Sphericity and roundness of proppants

In addition, grading of the proppant relates to the shape of the proppant in terms of filling void space. As one may recall the grading or size distribution of a proppant is defined as a certain fraction of the size particles falling through the largest mesh size and being held by the smallest. A quality grading of a 40/70 mesh proppant will provide a well distributed size of proppants between the two extremes. This allows for smaller particles to fill the void spaces that are found between the larger ones, providing support for the proppant pack. A study conducted by Mollanouri Shamsi et. al. (2018) revealed that a well graded proppant pack could have more conductivity over time, which disagreed with industry standards that a uniformly graded proppant was better. The final

findings of (Mollanouri Shamsi et. al., 2018) suggested that a well graded, medium angularity proppant pack will provide the best long-term results for hydraulic fracturing. However, for immediate testing of proppant, a highly round and spherical proppant will provide the highest conductivity.

The transportation of the proppant throughout the fracture network is arguably the most important variable to fracture conductivity and to a successful stimulation. If proppant is not well distributed throughout the fractures, all previous influences on conductivity do not matter. To place the proppant throughout the entire length of the fracture is no easy task. In order to get proppant to a location far from the wellbore, highly engineered fluids are utilized, as well as specific concentrations of the proppant. Immediately once the pumping of the slurry is stopped, the fracture begins to close. In a study conducted by Novotny (1977), it shows that this can take up to two hours. During this time, the proppant is settling, which in turn reduces the fracture width once it has fully closed, decreasing the fracture conductivity. As previously mentioned, slick-water is a commonly used fluid for stimulation, although it does not provide very good proppant transport. The use of nitrogen added to the fluid, as well as surfactants added to the fracturing fluid, can help improve the buoyancy of proppant, improving proppant distribution and the penetration to a far-reaching fracture tip (Boyer et. al, 2014).

As has been well defined, there are numerous shortcomings of propping agents during hydraulic fracturing. However, as the study of proppants has progressed, so has the ability of said newly developed proppants to outperform and overcome the shortfalls of common sand. The use of resin coated proppants, can improve proppant performance

as they are able to withstand much higher stresses than a standard quartz proppant. However, it is unreasonable to believe that a simple coating of the proppant can enhance its strength. A more likely explanation is that the resin inhibits fines migration, thus maintaining the proppant pack permeability (Weaver et. al, 2005). Surface modification agents such as non-hardening resins have provided tremendous results regarding the maintaining of fracture conductivity, as seen in Figure 1.3. Production rates from wells that are not utilizing surface modification agents have experienced a much greater decline, than those that are.

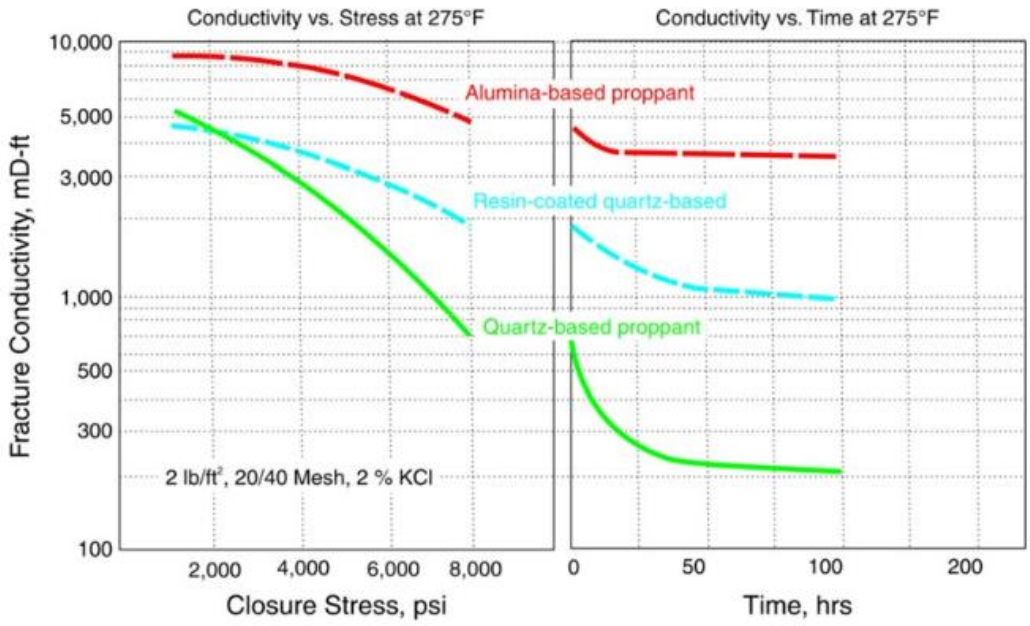

Figure 1.3 Effects on conductivity by surface modification agents applied to proppants

Another alternative to natural sand is sintered bauxite, which is a proppant that can withstand extremely high stresses. Sintered bauxite was first introduced in 1976, after extensive research was conducted by Cooke (Atteberry et. al., 1979). It was found that sintered bauxite can also provide an improvement in flow capacity compared to that of sand. When comparing the density of sand, sintered bauxite is nearly 1.5 times as dense, thus a more viscous and expensive fracturing fluid must be used. While there are many benefits to fracture conductivity and thus stimulation when sintered bauxite is used, the egregious rise in costs does not warrant its use for low permeability reservoirs.

Propping agent selection must be considered for every hydraulic fracture stimulation, as conditions are never the same. In order to get the most effective stimulation treatment, engineers must decide between a wide variety of proppants, fracturing fluids, and pumps in order to find the most effective treatment for any given well. The conditions of the proppant that would allow for successful stimulation in a shale reservoir is the one in which the proppant is of smaller size, medium angularity, and has a high crush strength. Economides and Nolte (2000) discussed the best proppant to be used for a range of closure stresses. They recommend sand as the propping agent for a closure stress of less than 6,000 psi, resin coated sand for closure stresses ranging between 6,000 and 12,000 psi, and sintered bauxite for closure stresses above 12,000 psi. As well, a fluid with appropriate viscosity should be used to allow for the best proppant transport possible.

1.3 Objective of Study

The objective of this study is to evaluate both local and premium sand proppants, as well as a possible substitute in taconite tailings, for their respective fracture conductivity. This will then provide insight as to the feasibility of using these respective proppants for future fracture treatments. While by no means is this study an economic analysis, a comparison of a locally sourced proppant versus that of one that must be brought to location, can provide a possible cost saving method. As well, the testing of a different material proppant altogether, may also provide a cost saving method.

2. EXPERIMENTAL DESIGN AND METHODOLOGY

2.1 Proppant Pack Conductivity Testing

This section outlines the required procedures to conduct a fracture conductivity test utilizing steel plates.

2.1.1 Experimental Setup

The components that are listed below are part of the experimental setup required to conduct the experiment.

1. Test Fluid Source (Nitrogen gas)
2. Gas Flow Meter
3. GCTS Hydraulic Press
4. Modified API Test Cell
5. Cell and Differential Pressure Sensors
6. Back Flow Regulator Valve

The experimental apparatus used for conductivity tests is shown in Figure 2.1.

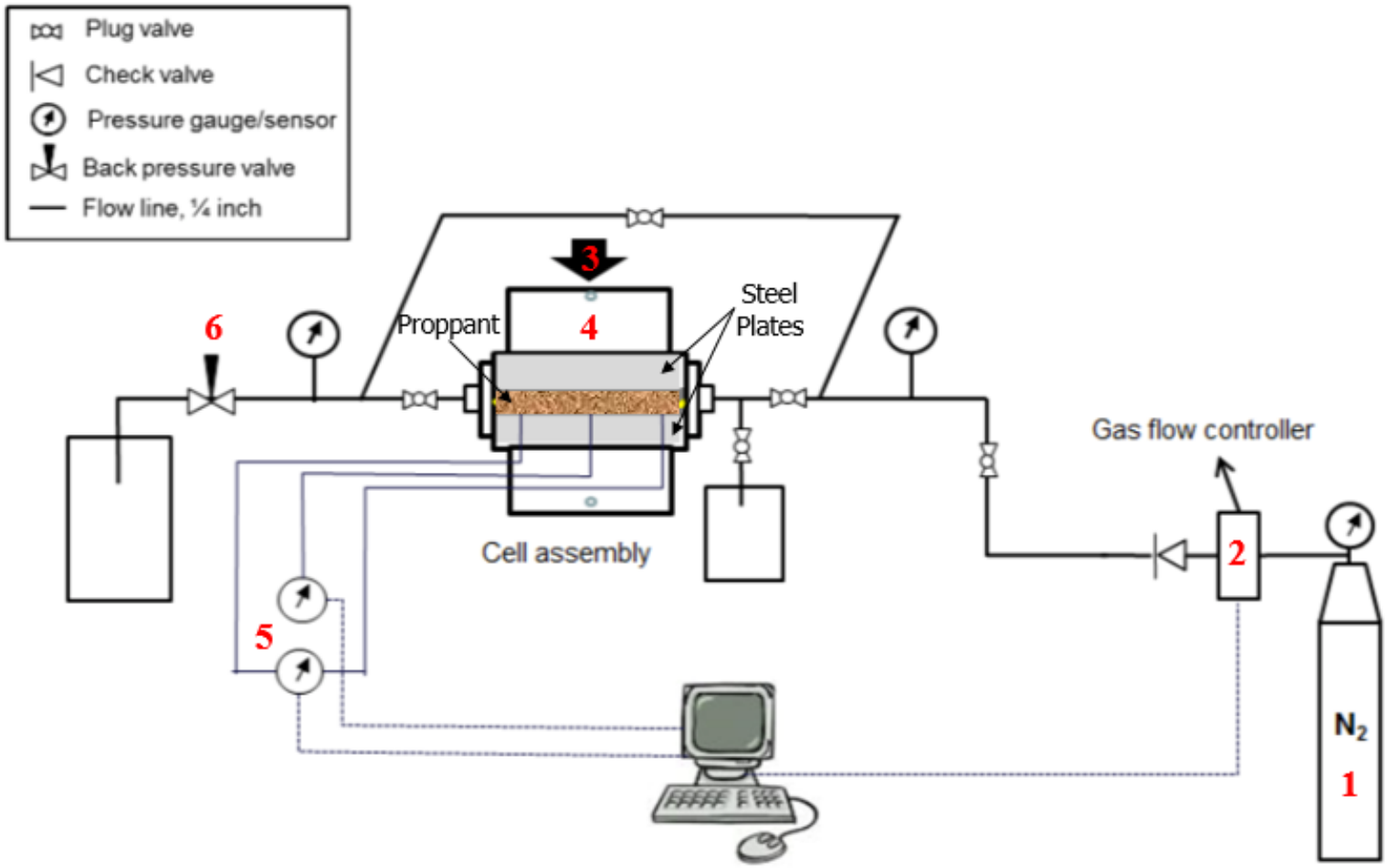

Figure 2.1 Test Setup Schematic

2.2 Preparation of Conductivity Sample

This section will discuss the preparation of the sample that was used for conductivity test. All tests were conducted under idealized conditions, utilizing only steel plates. Thus, only the preparation of steel plates and not core, will be discussed.

2.2.1 Testing Sample Design

To consistently evaluate proppant, excluding the effects of rock surfaces, steel plates were used. These steel plates are in accordance with the API RP 61 procedure for testing short term proppant packs. The steel plates are 1 inch thick and were designed to fit within tolerance of the API Conductivity Test Cell. They were manufactured at Texas A&M University.

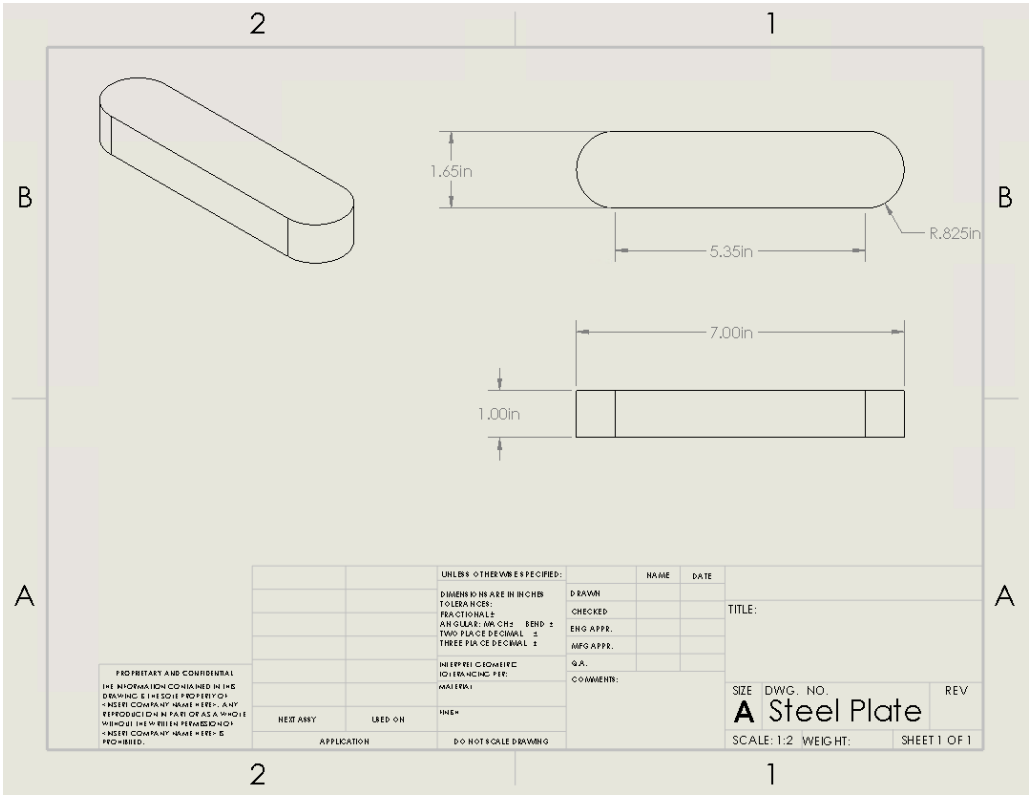

Figure 2.2 Blueprint schematic of individual steel plate member

2.2.2 Testing Sample Assembly

The steel plates consist of three 1-inch thick members that are glued together. A total of 6 members were manufactured, resulting in a total of two steel plates. These two sets of plates are what allow for the formation of the proppant pack, as a steel plate is providing both top and bottom support. As well, the steel plates, with the help of a sealing epoxy, allow for a tolerance that will inhibit the loss of proppant or gas leak-off, being that the mold is .003 inches wider than the conductivity cell. The steel plates are what allow for the closure stress to be applied to the proppant pack, acting as medium with the hydraulic press.

Figure 2.3 Assembled steel plate

2.2.3 Testing Sample Preparation Procedure

The preparation of the steel plates for use in the conductivity test cell assumes that three individual members have been molded to create one metal plate. The steel plate procedure is the same for both the bottom and top metal plate.

1. Apply a thin layer of Gorilla Glue to the top, middle, and bottom of the steel plate.
2. Place one layer of masking tape onto the outer layer of the metal plate and make sure it is flush with the surface. (attempt to minimize overlapping tape as tolerance can become an issue)
3. Apply another thin layer of Gorilla Glue on outside of masking tape and let completely dry.
4. Softly use steel wool to scratch the glue on the outside of the masking tape, creating dimension on the surface that allows for the better binding of epoxy.
5. Apply Momentive SS4155 Primer to masking tape surface of steel plate. Allow to dry for fifteen minutes or until surface becomes white. Repeat this process three times.
6. Clean all surfaces of metal mold.
7. Apply EZ Aluminum Tape onto side walls of metal mold. (This minimizes the width of the sample when epoxy is applied, maintaining tolerance, and allowing for a snug fit into conductivity cell.)

8. Spray Silicon Mold Release to the aluminum tape surface. Allow to dry for five minutes. Repeat this process three times. (Silicon Mold Release helps to reduce shear stress when removing sample from mold.)
9. Place sample evenly within the mold to ensure that an equal layer of epoxy is found on all sides of the sample.
10. Tighten all sides of mold with screws.
11. Mix Momentive RTV627 parts A and B using equal weight ratios. (For steel plate sample use 50 grams of both.)
12. Pour Momentive RTV627 Mixture from one end of sample, at a very slow rate. (This helps to reduce the formation of air bubbles in the epoxy, which can put into question the integrity of the epoxy. Pouring of the mixture should take between 15-20 minutes.)
13. Place mold in oven for four hours at a temperature of 120° F
14. Remove all screws from mold.
15. Remove one side and bottom of mold.
16. Use hydraulic press to shear sample from remaining side of mold.

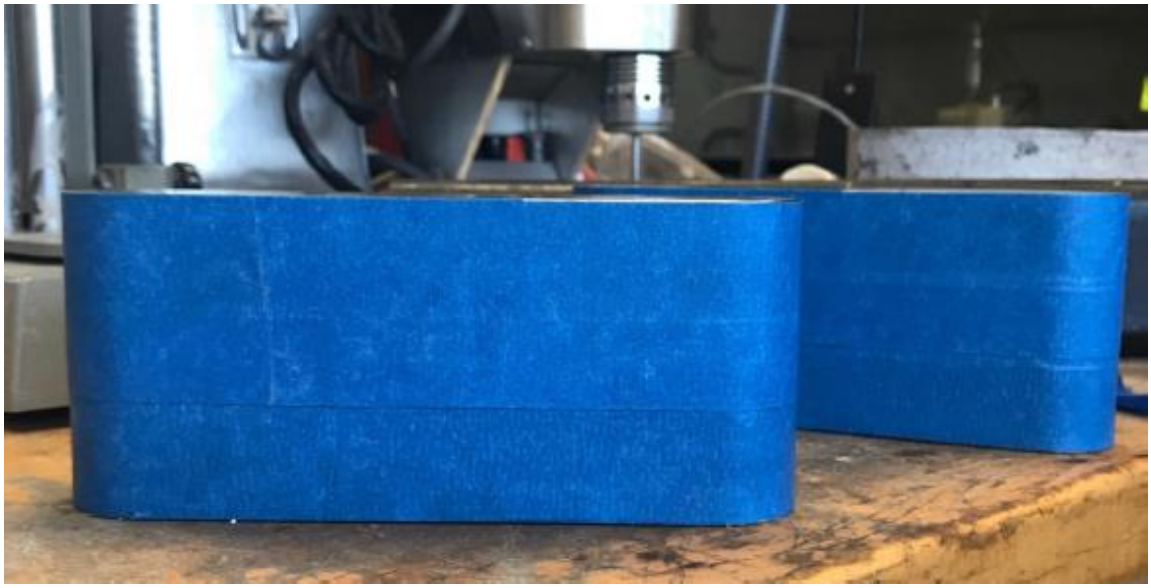

Figure 2.4 Steel plate with masking tape applied to outside surface (Wylie, 2018)

Figure 2.5 Steel plate with rubber epoxy surface applied to outside surface (Wylie, 2018)

2.3 Experimental Procedure

This experimental procedure assumes that the conductivity sample has been successfully placed within the cell. The conductivity test is now ready to be conducted following the procedure below.

1. Calibrate differential pressure sensors utilizing pressure pump and GTCS Software (2 Point option).
2. Verify that the back-pressure regulator is completely open in order to release air that may be trapped within the proppant pack.
3. Increase closure stress to the initial value (1000 psi).
4. Tighten all fittings.
5. Zero both the differential and cell pressure sensors.
6. Close back pressure regulator.
7. Start increasing gas flow rate with small increments carefully (flow rate should not surpass .2 L/min).
8. Continue to allow flow of gas until cell pressure reaches 30 psi.
9. Check for any leaks (cell pressure should be maintained at 30 psi and flow rate should settle at 0 L/min).

    If criteria is not met, search for leaks by applying soap solutions (leak will be indicated by bubbles forming where flow is being released).
10. Open back pressure regulator, increasing flow rate (do not increase past 2 L/min as this begins to approach Non-Darcy Flow).

11. Continue to increase flow rate. Ensure cell pressure is not reaching below 26 psi and differential pressure is not above 1.2 psi (pressures beyond these limits can uncalibrate pressure sensors).
12. A differential pressure that can provide four evenly distributed data points should be reached.
13. Record flow rate, cell pressure, and differential pressure.
14. Slowly decrease flow rate until the next differential pressure point is 3/4 of the original.
15. Record flow rate, cell pressure, and differential pressure.
16. Slowly decrease flow rate until the next differential pressure point is 1/2 of the original.
17. Record flow rate, cell pressure, and differential pressure.
18. Slowly decrease flow rate until the next differential pressure point is 1/4 of the original.
19. Record flow rate, cell pressure, and differential pressure.
20. Reduce gas flow rate until pressure gauge on Nitrogen tank reads 0 psi.
21. Open back pressure regulator once cell pressure is under 10 psi.
22. Allow all gas to escape conductivity cell, resulting in a cell pressure of 0 psi.
23. When cell pressure reaches 0 psi, increase closure stress to new desired closure stress.
24. Repeat steps 6-23 for new closure stresses at 2000 psi, 3000 psi, 4000 psi, 5000 psi, and 6000 psi.

25. Reduce closure stress to 1000 psi
26. Untighten all fittings.
27. Reduce closure stress to 0 psi.
28. Unload test cell from hydraulic press.
29. Disassemble test cell, remove sample, and collect proppant for post-crush sieve analysis.

2.4 Proppant Evaluation

2.4.1 Sieve Analysis of Proppant

A sieve analysis for the variation of proppants was used in order to confirm the range of sizes for the sand proppants or to create a mesh size altogether for the taconite tailings. Prior to the measurement of any proppant, the sieves were weighed independently. A mass of proppant is then weighed and put into the top sieve mesh. The range of meshes commonly used for the sand proppant were between 20 mesh and 100 mesh. A smaller mesh size was used for the taconite tailings ranging from 40 mesh to 170 mesh. The sieve test would be conducted for ten minutes to guarantee that the proppant successfully traveled through all mesh sizes until being withheld by a mesh size that was too small for the proppant to fall through. Figure 2.6 shows the size distribution of a Schlumberger 30/50 mesh sand proppant prior to testing.

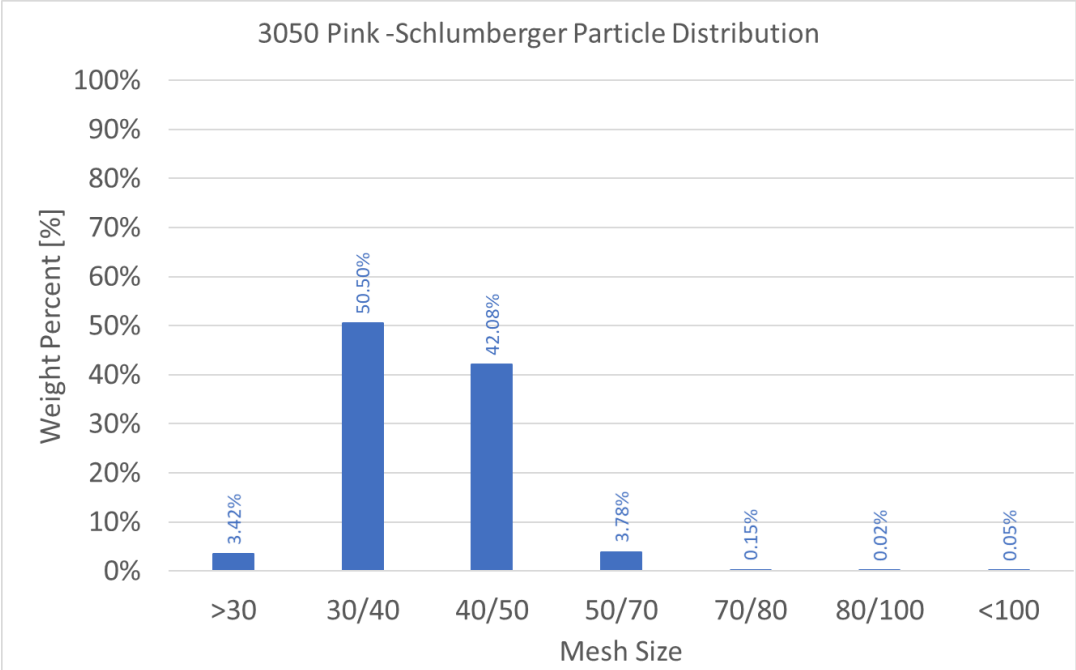

Figure 2.6 Example of 3050 mesh size distribution prior to crushing

Once completed, all sieves are weighed again. To guarantee a quality test, the mass of the proppant after the test would be compared to that prior to the test. The weights of both should be very close. The mass that was held by any given sieve was calculated by subtracting the pre-test weight of the sieve from the post-test weight of the sieve. This weight would then be divided by the total initial weight of the proppant, allowing for a distribution of weights from each sieve to be found. The distribution is expressed in percentage of total weight, as displayed in Figure 2.7. The downfall of this crushing test is that it is unable to identify at which closure stress crushing occurred. As well, it is unable to determine if a given particle has undergone crushing or if it was just initially on the smaller end of the mesh spectrum.

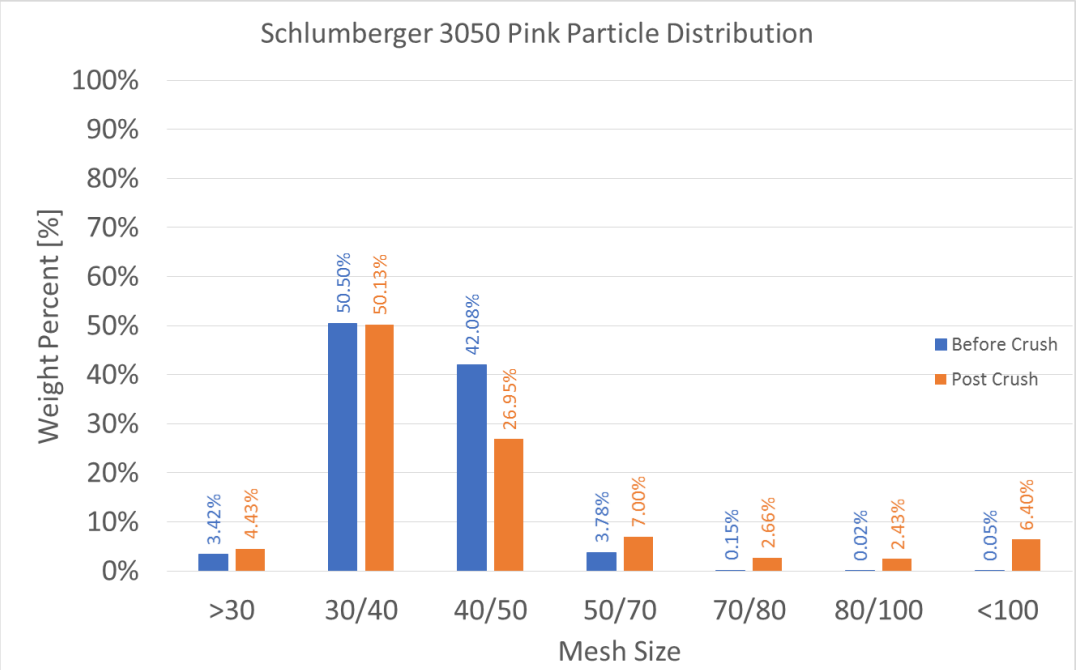

Figure 2.7 Example of 3050 mesh size distribution after crushing

2.4.2 Proppant Placement

Per the recommendation of API RP 61, a volume corresponding to a quarter inch proppant pack should be used for the fracture conductivity testing of a short term proppant pack. A quarter inch proppant, which relates to a 2 $\frac{lb}{in^2}$ proppant pack loading, is equivalent to 2.74 in^3 of any proppant for this given test cell. This volume can be calculated based on the blueprints provided in Figure 2.2, which represents an area of 10.966in^2.

In order to find the mass that relates to said volume, the density of each proppant must be measured. A 25 mL graduated cylinder is used. Ten sample weights of the graduated cylinder when filled is measured and an average of the mass is calculated. From here, the density of the proppant can be calculated. Knowing both the average

density of the proppant, as well as the volume of proppant that is necessary for a quarter inch proppant pack, the required mass can be calculated. This procedure was conducted for all proppants used.

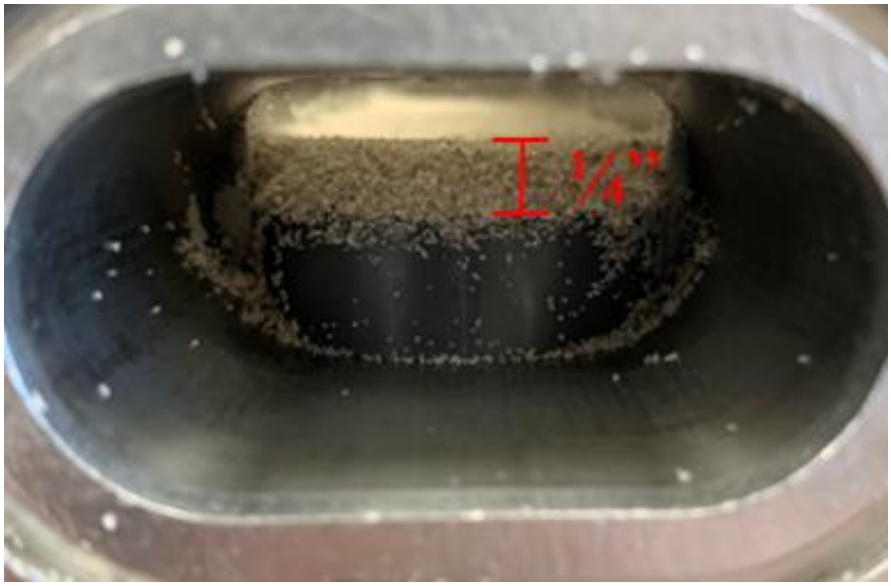

Figure 2.8 Side view of ¼” Proppant Pack used for idealized conductivity testing

The placing of the proppant requires the bottom steel plate and the bottom piston be put in place. The top of the bottom steel plate should be below the pressure ports because a clear path to the proppant pack is necessary when measuring the differential and cell pressure. API RP 61 recommends the placements of a mesh filter in all fluid entry and exit ports, as to contain all proppant. A funnel is then used to distribute the proppant from above, onto the top face of the steel plate. At this point, the sand is not compacted or very even. A flat surface should be used to compress the sand, resulting in an evenly distributed quarter inch proppant pack. Measurements are taken across the surface of the proppant pack to guarantee the equal distribution of the proppant.

Figure 2.9 Top view of ¼” Proppant Pack evenly distributed

All fittings are tightened to prevent the blowout of proppant, the top steel plate and the top piston will be placed into the API Conductivity Cell, and the initial closure stress of 1000 psi will be initiated. The final setup is reflected in Figure 2.10.

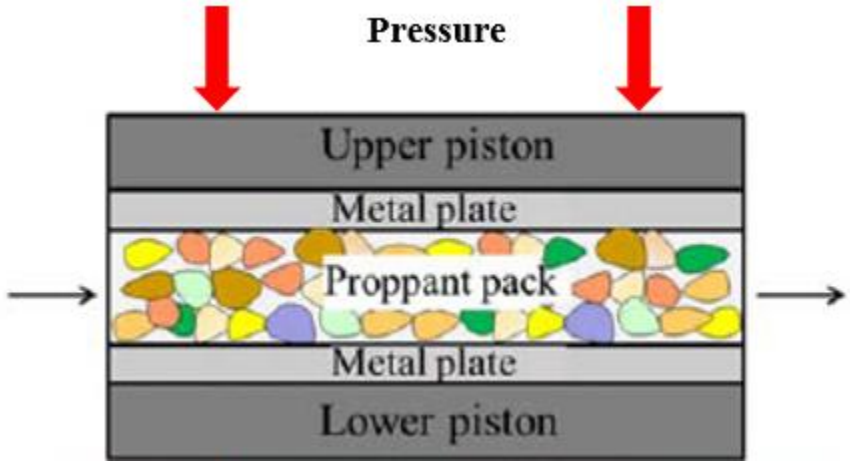

Figure 2.10 Complete setup of test cell with pressure being applied

2.5 Fracture Conductivity Calculation

Fracture Conductivity of a proppant pack is determined based on two equation, the Forchheimer equation and the Darcy Equation. The use of these two equations have independent stipulations for use. Darcy flow for a proppant pack is considered at flow rates less than 2 L/min (McGinley, 2015). For flow rates above 2 L/min, the use of the Forchheimer equation is suggested. The experiments conducted are based solely on the derivation of the Darcy equation being that flow rates rarely exceeded 1 L/min. The Darcy equation is shown in Eq. 2-1

$$-\frac{dp*k_f}{dl*\mu} = v = \frac{q}{A} \tag{2.1}$$

The pressure drop measured over a unit length is defined by $-\frac{dp}{dl}$, μ is the fluid viscosity, v is the fluid velocity, and k_f is the permeability of the fracture. Utilizing the measurements from the experiment requires the combination of the Darcy's Law and the ideal gas law. Equation 2.1 must be multiplied by the fluid density, ρ_f.

$$-\frac{dp}{dl}\rho_f = \frac{\mu v}{\text{kf}}\rho_f \tag{2.2}$$

The ideal gas law is defined as,

$$pv = nRT \tag{2.3}$$

However, when considering the fluid density, the real gas law is

$$pM = ZRT\frac{m}{v}ZRT\rho_f \tag{2.4}$$

$$\rho_f = \frac{pM_g}{ZRT} \tag{2.5}$$

In Equation 2.5, (ρf) is the fluid density, (p) is the pressure, (M_g) is the gas molecular weight, (R) is the gas constant equal to 8.334, (T) is the temperature in Kelvin, and (Z) is the gas compressibility factor. The cross sectional area is defined as

$$A = wh \tag{2.6}$$

Incorporating Equation 2.5 and Equation 2.6 into the left side of Equation 2.2 and manipulating, we obtain Eq. 2.7.

$$-\frac{pM_g}{ZRT}dp = \frac{\mu}{k_f w_f h_f} q\rho_f dL \tag{2.7}$$

Integrating Equation 2.7, we obtain Eq. 2.8

$$\frac{(p_1^2-p_2^2)}{2}\frac{M_g}{ZRT} = \frac{\mu}{k_f w_f h_f} q\rho_f L \tag{2.8}$$

Rearranging Equation 2.8, we obtain

$$\frac{(p_1^2-p_2^2)}{2L}\frac{M_g}{ZRT} = \frac{\mu q \rho_f}{h_f}\frac{1}{k_f w_f} \tag{2.9}$$

p_1 is defined as the pressure upstream from the pressure sensor, while p_2 is defined as the pressure below it. L is the length of the flow path, between the differential pressure sensors. q is the flow rate of the gas entering the proppant pack, w_f is the fracture width, which is a quarter inch for the testing of a short-term proppant pack as defined by API RP 61, and h_f is the width of the sample which is 1.65 inches. It must be assumed that the first half of the differential pressure measurement is equal to the second half, thus allowing p_1 and p_2 to be defined as,

$$p_1 = p_{CELL} + .5\Delta p \tag{2.10}$$

$$p_2 = p_{CELL} - .5\Delta p \tag{2.11}$$

Recall that the definition of fracture conductivity is the fracture width multiplied by the fracture permeability, thus $k_f w_f$ can be substituted by (C_f). As well, incorporating Equation 2.10 and Equation 2.11, Equation 2.9 becomes

$$\frac{[(p_{CELL}-.5\Delta p)^2-(p_{CELL}+.5\Delta p)^2]}{2L}\frac{M_g}{ZRT}=\frac{\mu q \rho_f}{h_f}\frac{1}{C_f} \tag{2.12}$$

Further simplification of Equation 2.12 results in

$$\frac{p_{CELL}\Delta p M_g}{LZRT}=\frac{\mu q p}{h_f}\frac{1}{C_f} \tag{2.13}$$

Equation 2.13 is the final equation needed in order to calculate the fracture conductivity through a proppant pack. There are three unknowns which are the flow rate of nitrogen gas (q), the cell pressure (p_{cell}), and the pressure drop along the length of the proppant pack (Δp). The molecular weight (M_g), the compressibility factor (Z), the density (ρ_f), and the viscosity (μ) are all properties of the fluid, in this case, nitrogen. (L) and (h_f) are known and have been previously mentioned. Four data points are taken at each closure stress. The slope of all four data points are taken into account by plotting $\frac{p_{CELL}\Delta p M}{LZRT}$ vs $\frac{\mu q p}{h}$. The inverse of this slope is fracture conductivity.

The units of Equation 2.13 are rather cumbersome and it can become difficult as to how exactly the units of conductivity were obtained. The units and all conversions will be simplified, beginning with the left-hand side (LHS) of Equation 2.12

$$\frac{[(p_{CELL}-.5\Delta p)^2-(p_{CELL}+.5\Delta p)^2]}{2L}\frac{M_g}{ZRT} \tag{2.14}$$

$$(LHS\ Units)*(Conversion\ Factors)$$

$$\left(\frac{Psi^2}{in}*\frac{\frac{Kg}{mol}}{\frac{J}{mol*K}*K}\right)*\left(\frac{6894.8^2*\frac{Pa^2}{Psi^2}}{\frac{.0254\ m}{in}}\right) \tag{2.15}$$

A Pascal is equal to $\frac{J}{m^3}$ and because the "psi" is squared, when converting to Pascals, it is necessary to also square this unit. For simplification of the equation, the square will be separated into $Pa*\frac{J}{m^3}$. Equation 2.16 is a further simplification of 2.15.

$$\left(\frac{Psi^2}{in}*\frac{\frac{Kg}{mol}}{\frac{J}{mol*K}}\frac{1}{K}\right)*\left(\frac{6894.8^2*\frac{Pa}{Psi^2}*\frac{J}{m^3}}{\frac{.0254\ m}{in}}\right) \tag{2.16}$$

The final units of the left-hand side (LHS) of Equation 2.12 are $\frac{Pa*Kg}{m^4}$.

A similar method will be used to clarify the right-hand side (RHS) of Equation 2.12.

$$\frac{\mu qp}{h_f} \tag{2.17}$$

$$(RHS\ Units)*(Conversion\ Factors)$$

$$\left(\frac{Pa*sec*L*\text{kg}}{min*m^3*in}\right)*\left(\frac{1\ min}{60\ sec}*\frac{1\ in}{.0254\ m}*\frac{.001\ m^3}{1\ L}\right) \tag{2.18}$$

The final units of the right-hand side (RHS) of Equation 2.12 are $\frac{Pa*Kg}{m}$.

When plotting the Left Hand Side vs the Right Hand Side of the equation, the resulting slope of Equation 2.19 will have units of (m^{-3}). The following conversion will result in the common units used for fracture conductivity ($md * ft$).

$$\frac{1}{C_f} = 5.02E^{12}\ (m^{-3}) \tag{2.19}$$

$$\frac{1}{C_f} = \frac{5.02E^{12}}{\cancel{m^2}} * \frac{9.86E^{-16}\ \cancel{m^2}}{md} * \frac{1\ \cancel{m}}{3.281\ ft} \tag{2.20}$$

$$Cf = 662\ (md\text{*ft}) \tag{2.21}$$

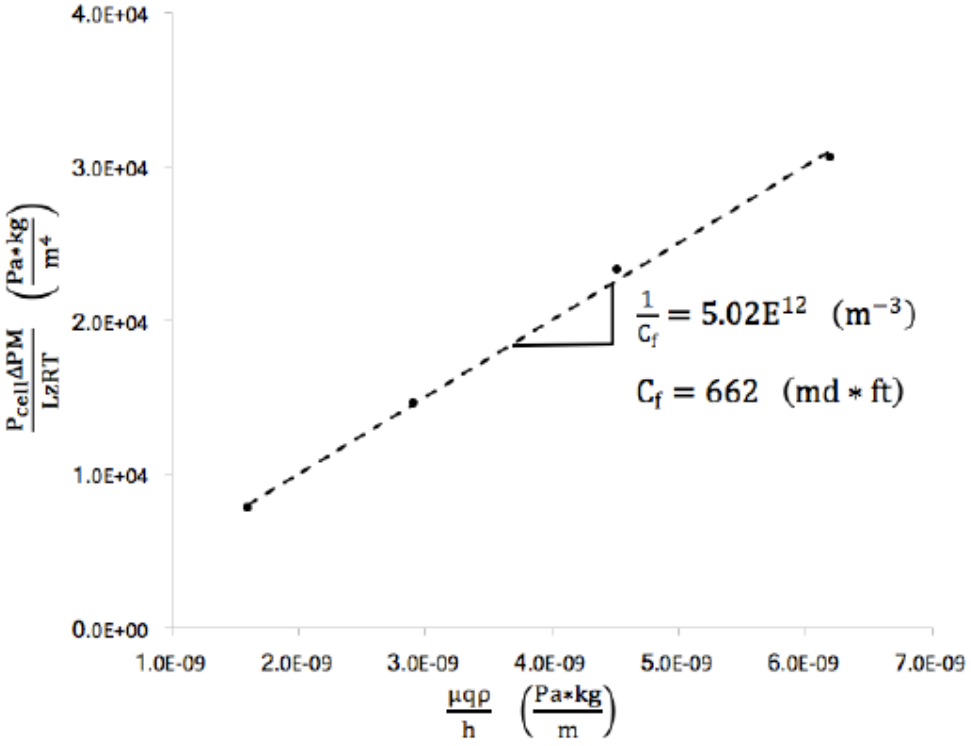

Figure 2.11 Experimental results used to determined conductivity of proppant pack (from Wylie, 2018)

3. RESULTS

The results of this study present the data for twenty different proppants ranging in size from 30/50 mesh to 100 mesh. The proppants were separated into five groups based on if they were sand or taconite, as well as their mesh size. Seven 100 mesh sand proppants, three 40/70 mesh sand proppants, and four 30/50 mesh sand proppants were tested. In addition, four 40/70 mesh taconite proppants and two 100 mesh taconite proppants were tested. Each proppant had at minimum two tests conducted in order to verify the results.

Proppant Number	Proppant Type	Proppant Name	Number of Tests Completed
1	100 Mesh Sand	HAL - Northern	2
2		HAL - Local	2
3		SLM - S012	2
4		SLM - Brown	2
5		SLM - White	2
6		HAL-Prem White Northern	2
7		HAL-Prem White Local	2
8	40/70 Mesh Sand	SLM - S012	2
9		SLM - Brown	2
10		SLM - White	2
11	30/50 Mesh Sand	HAL - Northern	2
12		SLM - Pink	2
13		SLM - Brown	2
14		SLM - Mix	2
15	40/70 Mesh Taconite	Keetac #1	2
16		Keetac #2	2
17		Keetac #3	2
18		Keetac #5	2
19	100 Mesh Taconite	Keetac #1	2
20		Keetac #2	2

Table 3.1 Testing Matrix

The results will be separated in terms of proppant type and mesh size. Many of the variables that were said to have an influence on fracture conductivity as discussed in the literature review, will be used to interpret the results. These include the size distribution or sorting, crushing, and the sphericity and roundness of each proppant. The percent crushing was evaluated by finding the difference in percentage of a range of particles within a given sieve distribution before and after a conductivity tests was completed. Unfortunately, the influence of proppant embedment and fines migration are unable to be tested. The fracture conductivity of all proppants was measured at six closure stresses ranging from 1000 psi to 6000 psi. While all remaining data is presented in the Appendix, if more than three types of proppant for the same mesh size were tested, only the results for the best, middle, and worst-case scenario are discussed, in this descending order. A microscopic view of each proppant is provided at a consistent 4X magnification, as well as a measurement of .5 millimeters provided in the bottom left of the view. A true comparison of size, shape, and roundness can be made amongst all proppants as the same condition was used throughout.

The sphericity and roundness of a proppant particle is determined by comparing said particle to a Krumbein and Sloss Chart found in Figure 3.1. This chart presents differing sphericity and roundness of particles in increments of 20%. The optimum proppant particle that will lead to the highest conductivity results will have near 90% sphericity and roundness. A visual comparison between the proppants and the chart

will be used to validate the fracture conductivity data, lending an idea as to why a certain proppant has better or worse results.

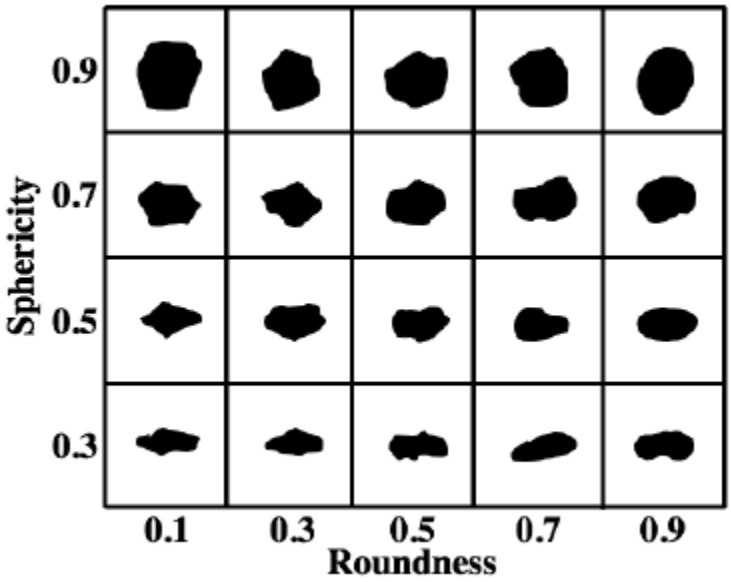

Figure 3.1 Krumbein and Sloss Chart

A general comparison of fracture conductivity results for all proppants tested can be seen in Figure 3.2. While proppants of the same size will not necessarily provide the same results, they tend to act in a similar manner. This is evident in the gathering of conductivity curves for a proppant that is of the same size, compared to those of a different size. The five groupings of the proppants, as has been previously defined, are associated with a certain color on the fracture conductivity curve which allows for the clear definition of results.

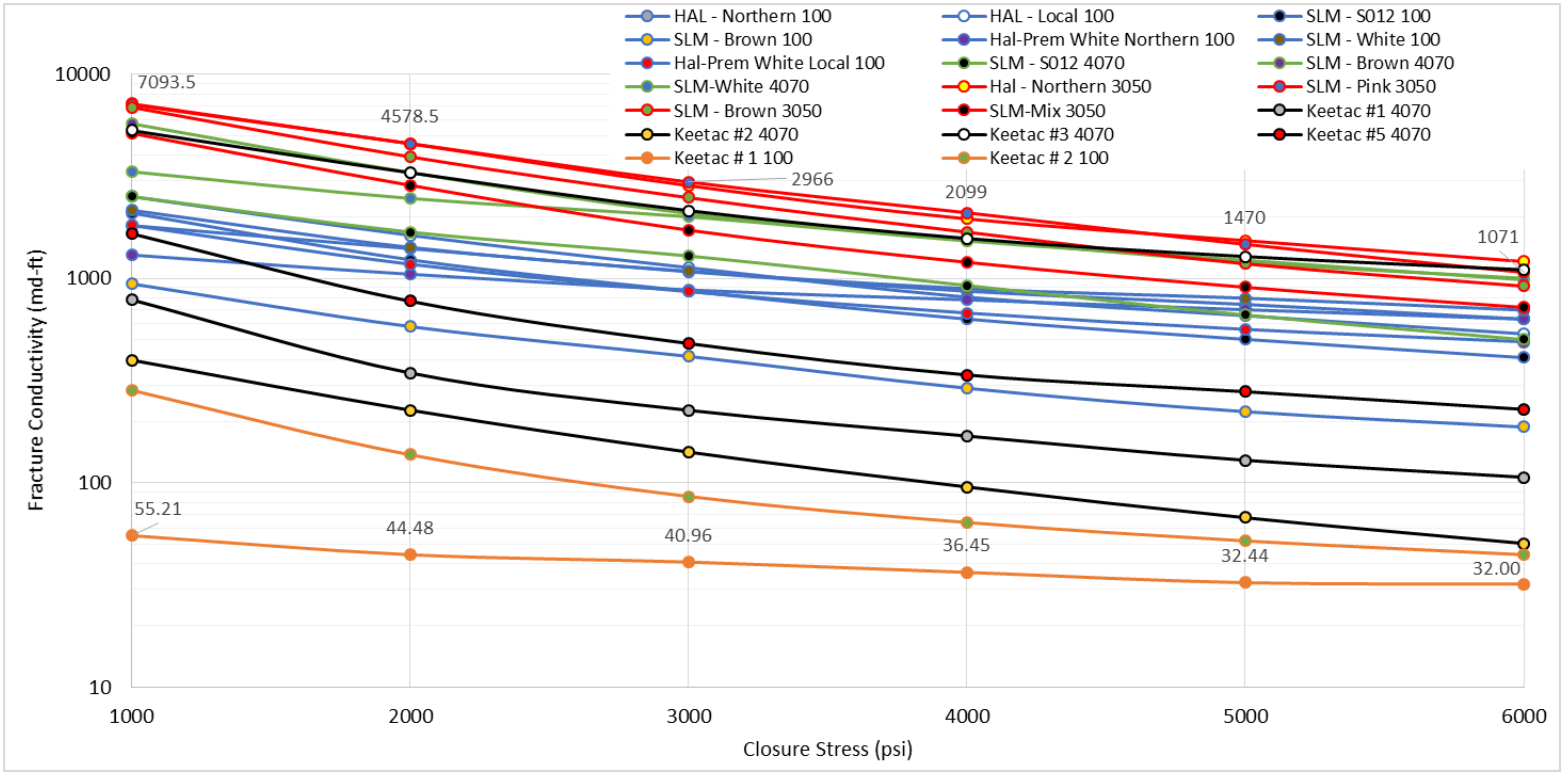

Figure 3.2 Fracture conductivity results of all proppants tested

3.1 Conventional Sand

A total of fourteen different sand proppants were tested in order to find their respective fracture conductivity. These proppants are reffered to as conventional sand because it is commonly used in hydraulic fracturing practices today. In contrast, the taconite that will be discussed is referred to as a novel proppant because testing of its viability as a proppant subsititute is in the elemntary stages. A wide variety of results were found within the subcategories of a given mesh size, such as a comparison between two idfferent proppants of a 30/50 mesh size. However, said mesh sizes provided results that were expected, when compared to other mesh sizes. Figure 3.3 presents the fracture conducitivty of only 30/50, 40/70, and 100 mesh sand proppants.

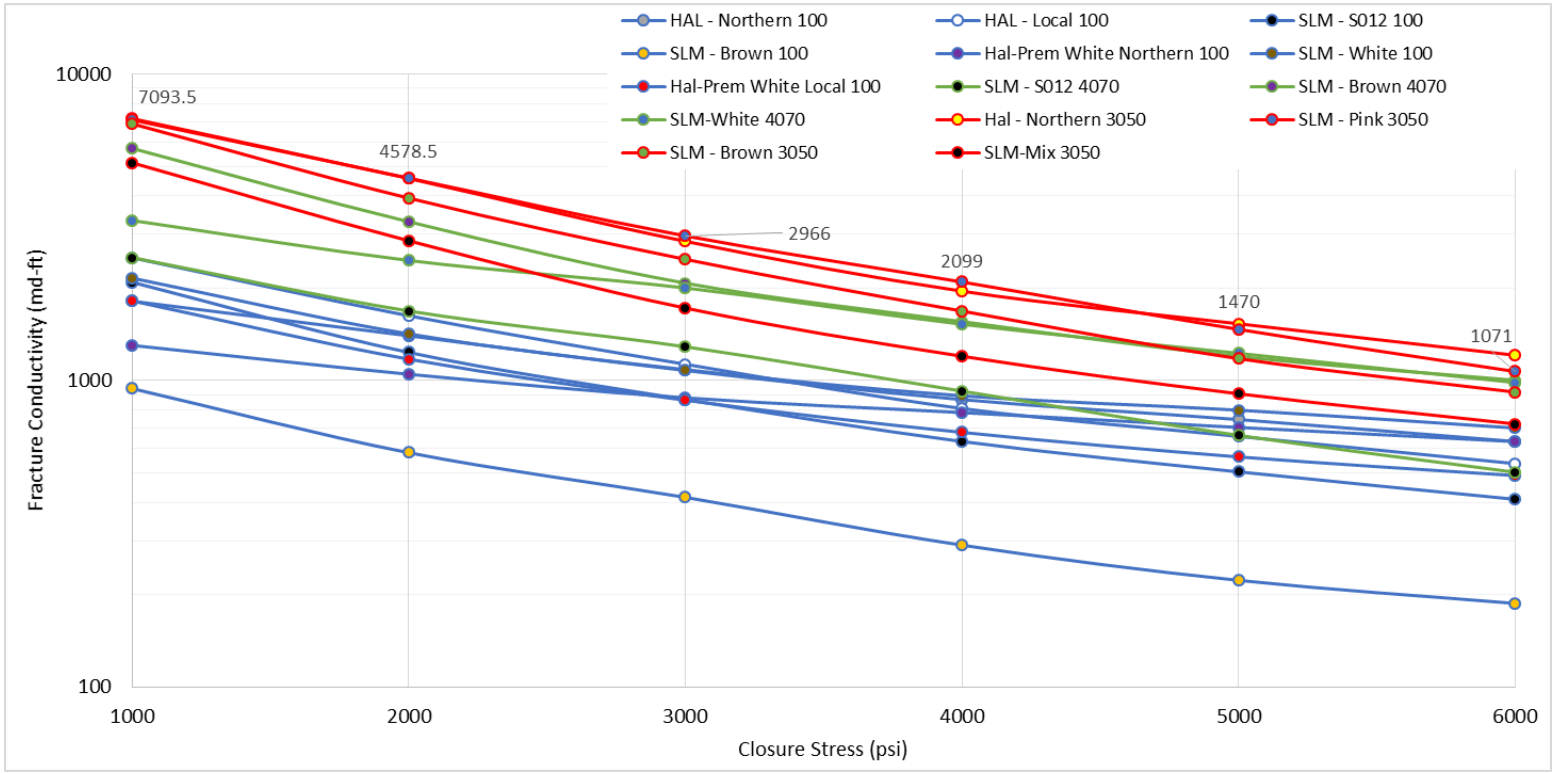

Figure 3.3 Fracture conductivity results of only sand proppants tested

3.1.1 30/50 Mesh

Proppant Number	Proppant Type	Proppant Name	Number of Tests Completed
11	30/50 Mesh Sand	HAL - Northern	2
13		SLM - Brown	2
14		SLM - Mix	2

Table 3.2 30/50 Mesh Sand Testing Matrix

3.1.1.1 Proppant Geometry

The proppant geometry of the 30/50 mesh sand for the best and middle case scenario are comparable in sphericity and roundness. Neither the Halliburton Northern nor the Schlumberger Brown proppants suffered from any extreme angularity. While no means are all particles spherical in shape, a large majority are. The Schlumberger Mixed proppant was far less spherical and had many more jagged edges when compared to the two other proppants. Based solely on proppant geometry, the first two proppants should have a higher conductivity than the last one.

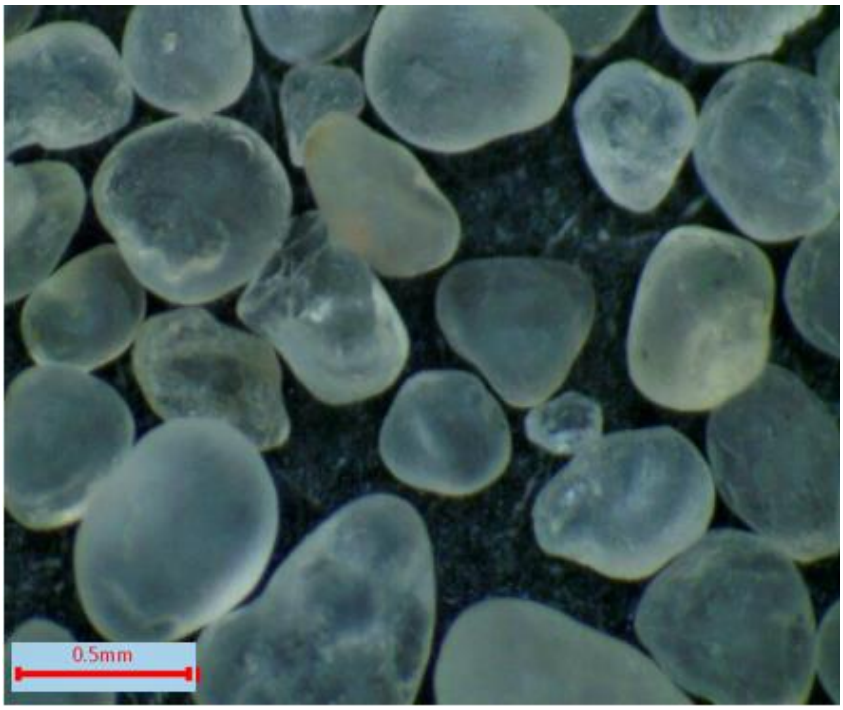

Figure 3.4 Magnification of Halliburton Northern 3050 Mesh

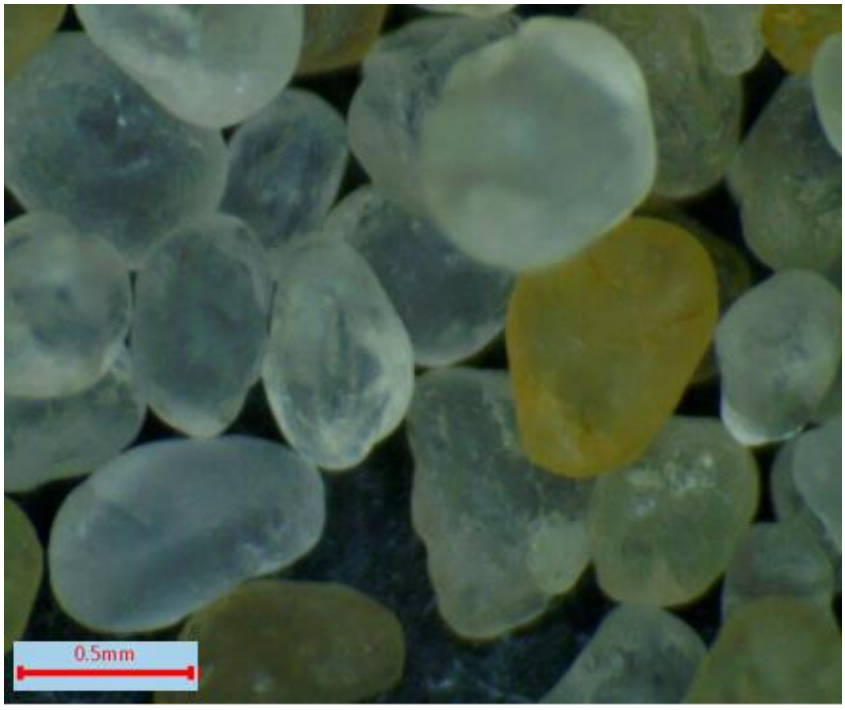

Figure 3.5 Magnification of Schlumberger Brown 3050 Mesh

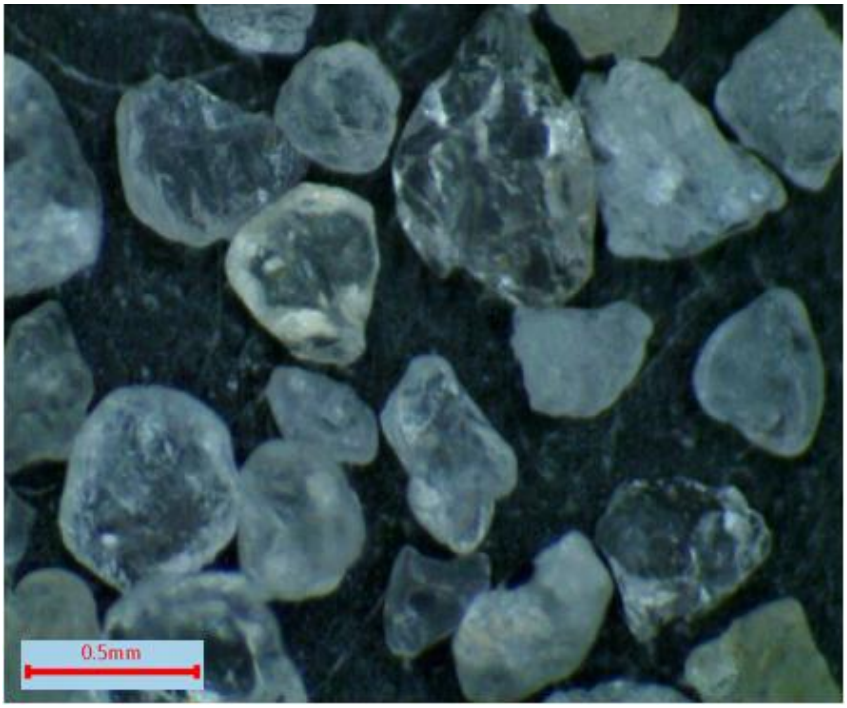

Figure 3.6 Magnification of Schlumberger Mix 3050 Mesh

3.1.1.2 Proppant Distribution and Crushing

The three different 30/50 mesh sand proppants all met the criteria that 90% of proppant fall through the 30 mesh screen and is withheld by the 50 mesh screen. This is to say that if all other criteria was the same, a similar first conductive data point could be expected. Halliburton Northern, which had the highest conductivity, had the lowest crushing percentage at only 4%. The middle case proppant, Schlumberger Brown, suffered from 9% crushing, while the Schlumberger Mix observed approximately 21% crushing. The crushing of proppant can be observed in the general trend of the conductivity curve. Based on crushing percentages, Halliburton Northern should have the highest conductivity at the end of the test, while the Schlumberger Mix should have the lowest. Crushing data is observed in Figures 3.7, 3.8, and 3.9.

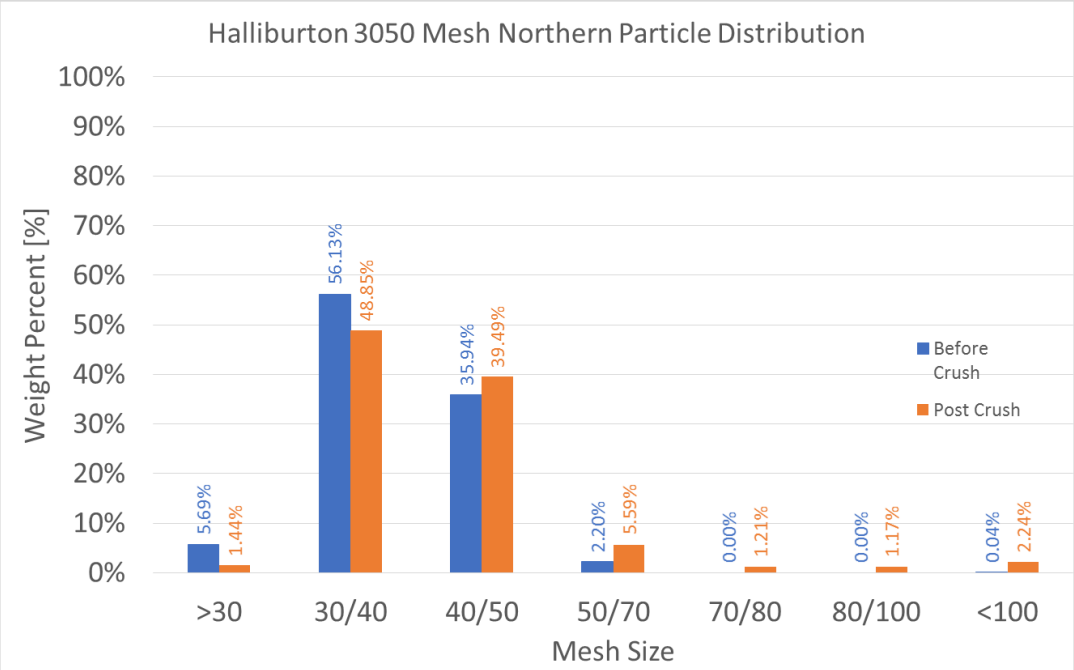

Figure 3.7 Size distribution of Halliburton Northern 3050 Mesh

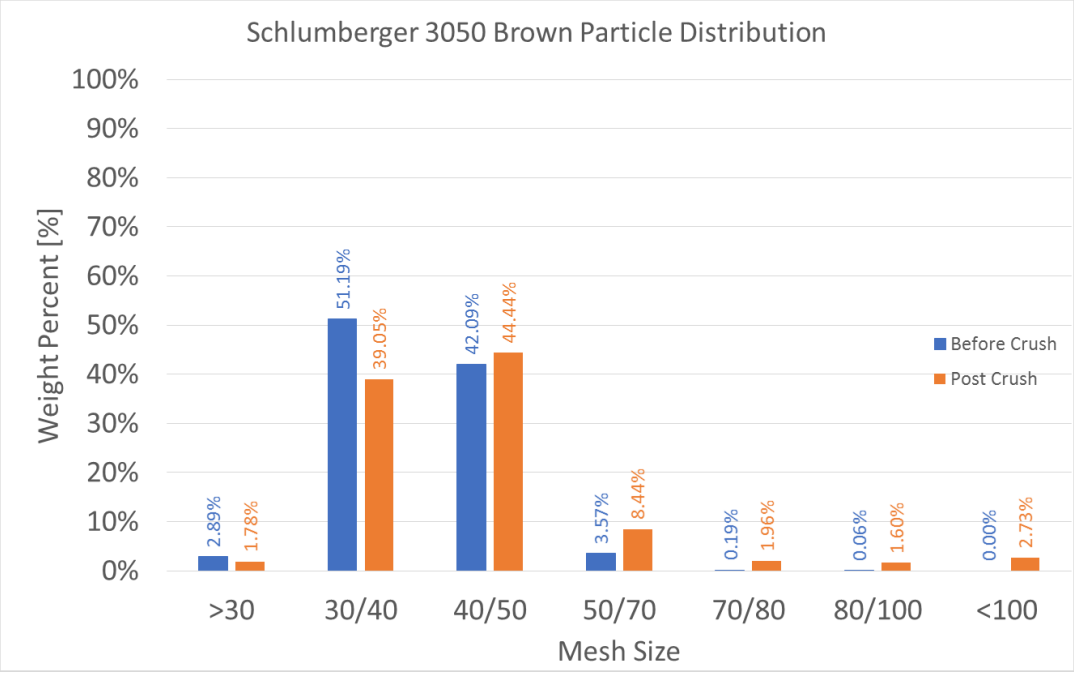

Figure 3.8 Size distribution of Schlumberger Brown 3050 Mesh

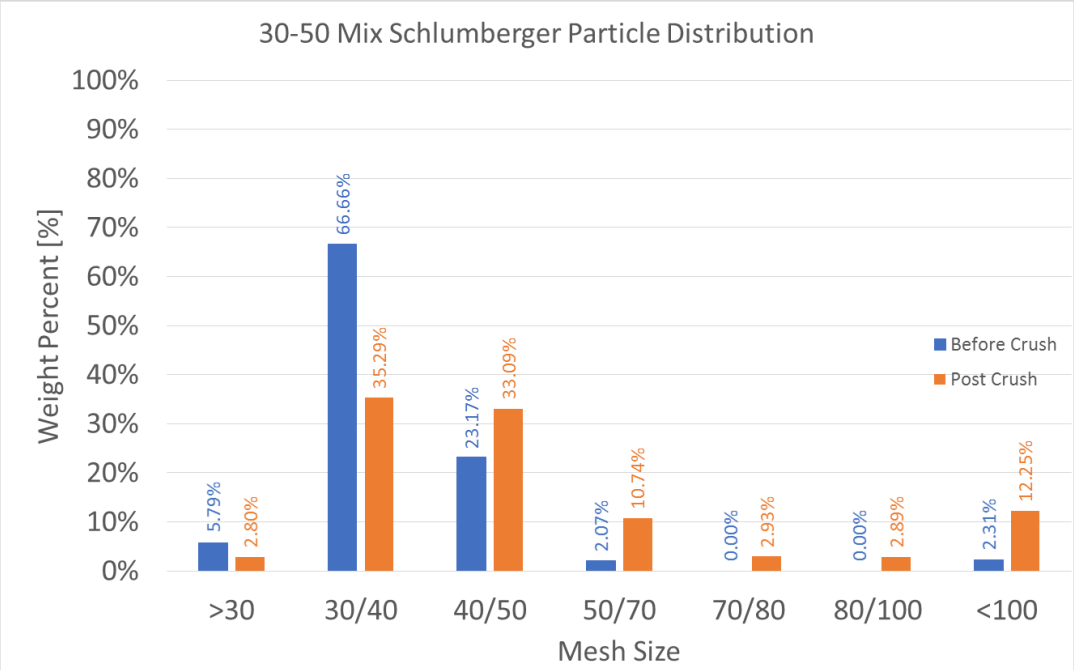

Figure 3.9 Size distribution of Schlumberger Mix 3050 Mesh

3.1.1.3 Fracture Conductivity

Figure 3.2 displays the conductivity results of the 30/50 proppant group compared to all other proppants. It is clear that the largest size proppant provided the highest fracture conductivity. This is to be expected being that a larger sized proppant particle will allow for a more permeable proppant pack. A closer look at only the 30/50 mesh sand proppants reveals that the shape and sphericity of the proppant, as well as the crushing percentage, had noticeable effects on the conductivity. Initial proppant size distribution is not believed to have had much effect on the results.

The disassociation from a spherical shape, with rounded edges is what likely caused the Schlumberger Mix proppant to have a much lower initial conductivity than the Halliburton Northern or the Schlumberger Brown. The somewhat triangular shape of

the proppant leads to voids being filled, reducing a path for flow within the proppant pack.

The effect of crushing on conductivity is quite evident in Figure 3.10. A decline in the conductivity curve is always to be expected because an increase in closure stress decreases the fracture width, however, the severity of said crushing will have an impact on the slope of this decline curve. Both Halliburton Northern and Schlumberger Brown had very close initial conductivity value, however Schlumberger Brown experienced a crushing that was 6% more. As such, the fracture conductivity observed as each closure is reduced compared to the Halliburton North proppant. Similarly, the Schlumberger Mix proppant experienced an even greater crushing percentage and thus, its conductivity data points are much lower.

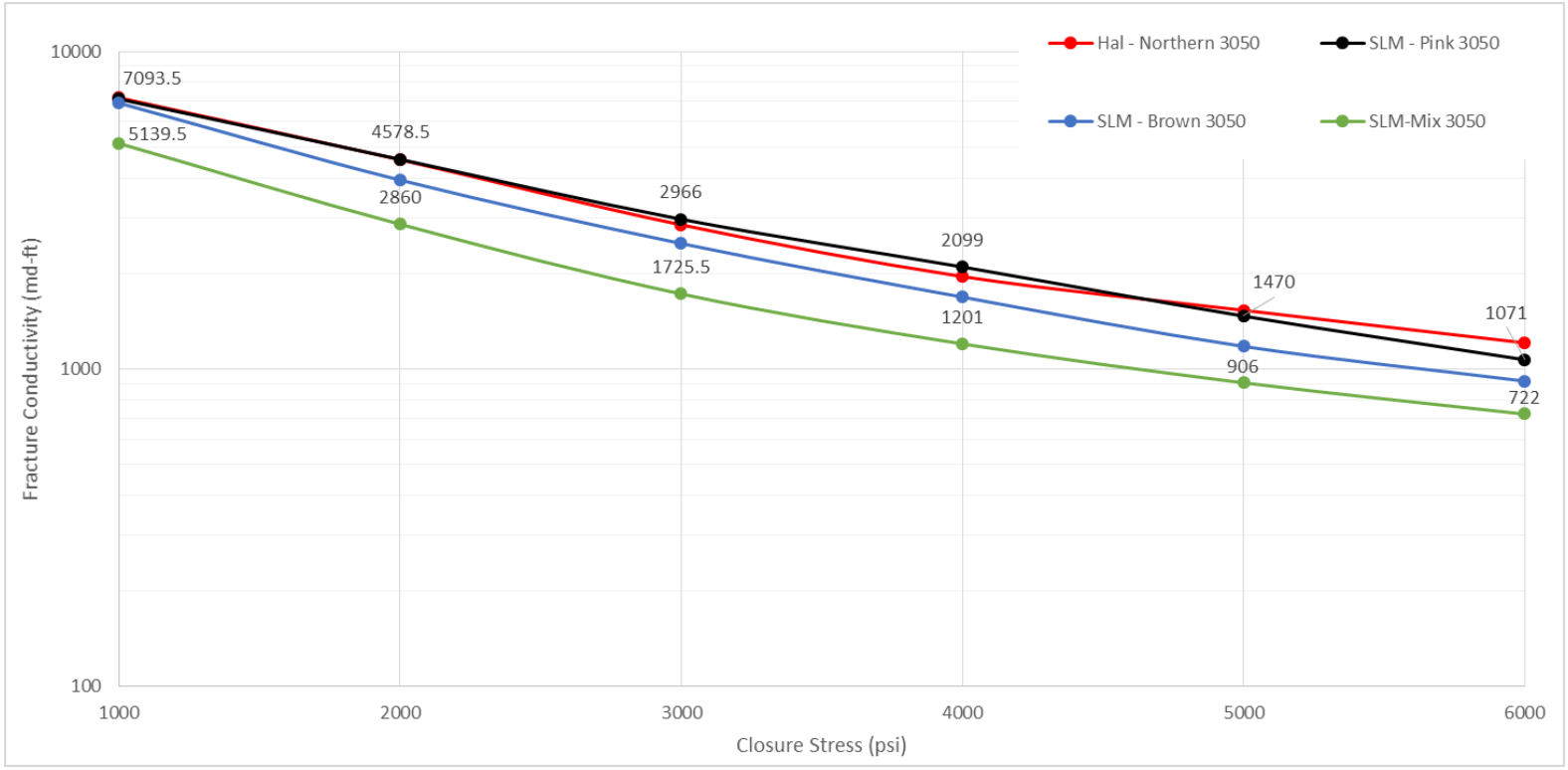

Figure 3.10 Fracture conductivity results of 3050 Mesh sand proppants tested

3.1.2 40/70 Mesh

Proppant Number	Proppant Type	Proppant Name	Number of Tests Completed
8	40/70 Mesh Sand	SLM - S012	2
9		SLM - Brown	2
10		SLM - White	2

Table 3.3 4070 Mesh Sand Testing Matrix

3.1.2.1 Proppant Geometry

The 40/70 mesh sand proppants saw quite the variation in sphericity and roundness. Schlumberger Brown 40/70 mesh, not to be mistaken as Schlumberger Brown 30/50, was fairly well rounded. However, it had a multitude of different shapes that cannot be identified as remotely spherical. Schlumberger White 40/70 was very similar in terms of roundness and again saw many differently shaped particles, including those that mimicked an ellipse. Schlumberger SO12 was much less spherical and had many more jagged edges. A microscopic view of each proppant can be seen in Figures 3.11, 3.12, and 3.13.

Figure 3.11 Magnification of Schlumberger Brown 4070 Mesh

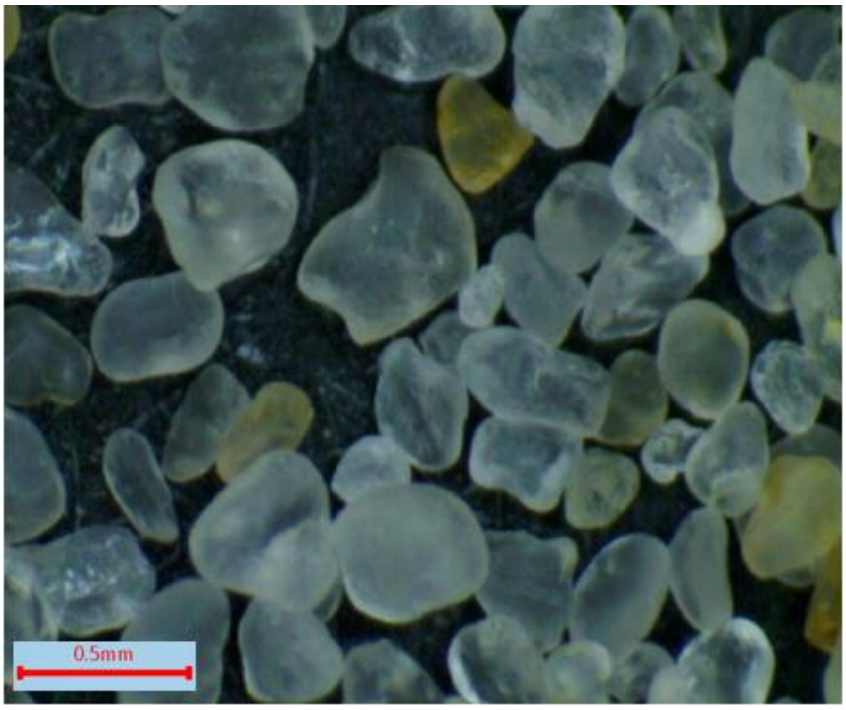

Figure 3.12 Magnification of Schlumberger White 4070 Mesh

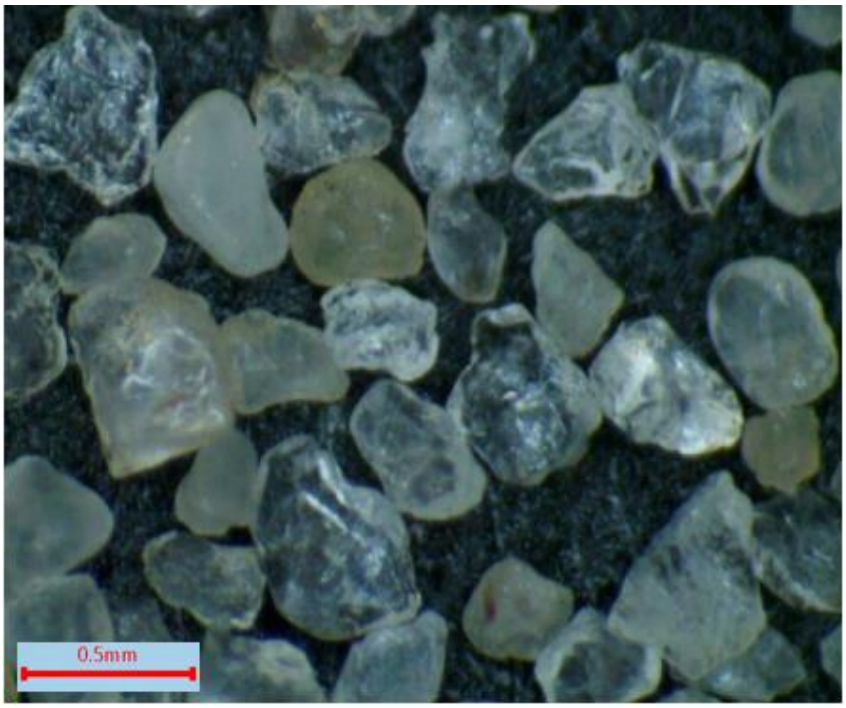

Figure 3.13 Magnification of Schlumberger SO12 4070 Mesh

3.1.2.2 Proppant Distribution and Crushing

The three proppants discussed all met the 90% proppant distribution criteria. When comparing the Schlumberger Brown and White proppants, Schlumberger White has a slightly smaller size distribution. This could result in a lower conductivity value at the initial closure stress. Schlumberger SO12 had a 96% pre crush proppant distribution between 40 mesh and 70 mesh, which is the same as Schlumberger Brown. Thus, if proppant shape was similar, the first conductivity data point should be similar to Schlumberger White. Both Schlumberger Brown and White had relatively low crushing percentages at 12% and 9% respectively. Meanwhile, Schlumberger SO12 had a crushing percentage of 21%. Proppant crushing leads to a reduction in fracture conductivity.

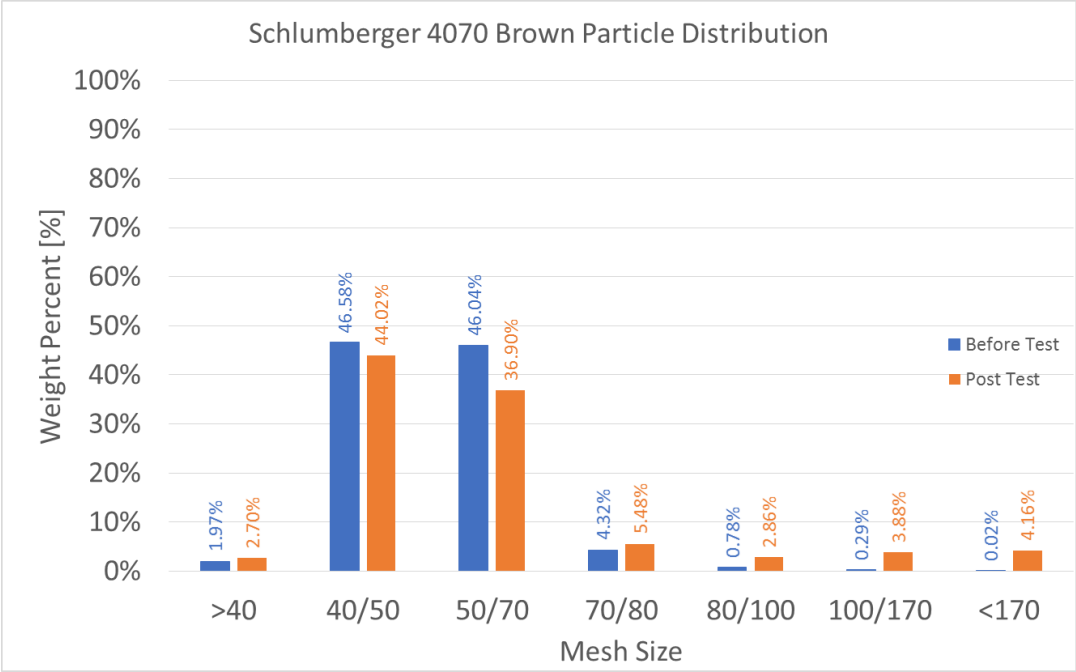

Figure 3.14 Size distribution of Schlumberger Brown 4070 Mesh

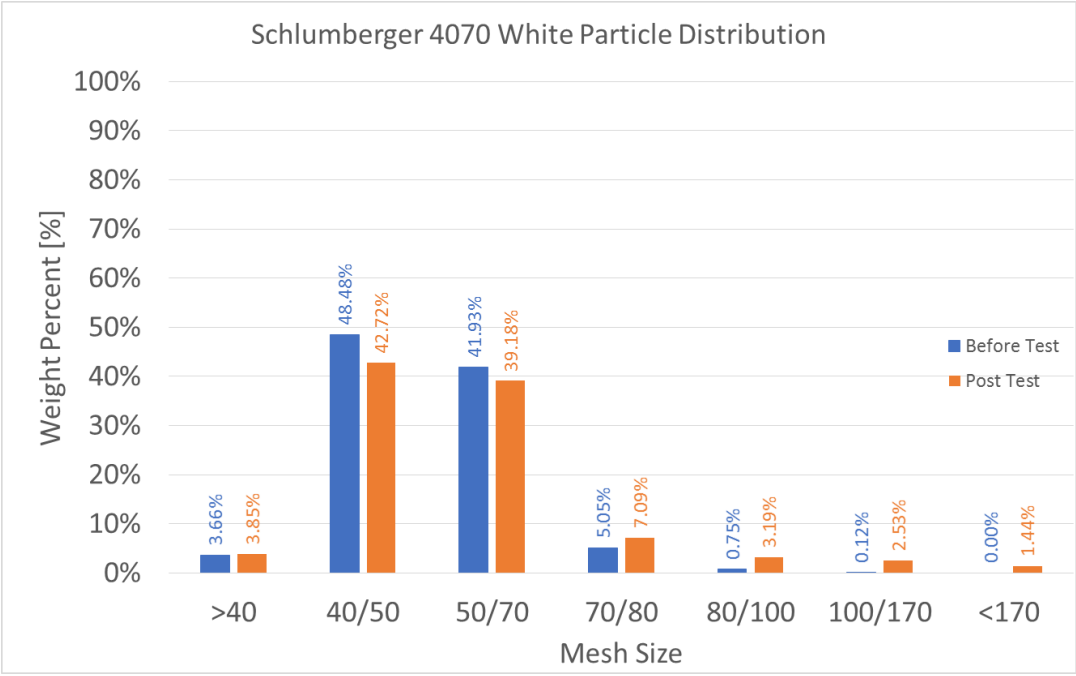

Figure 3.15 Size distribution of Schlumberger White 4070 Mesh

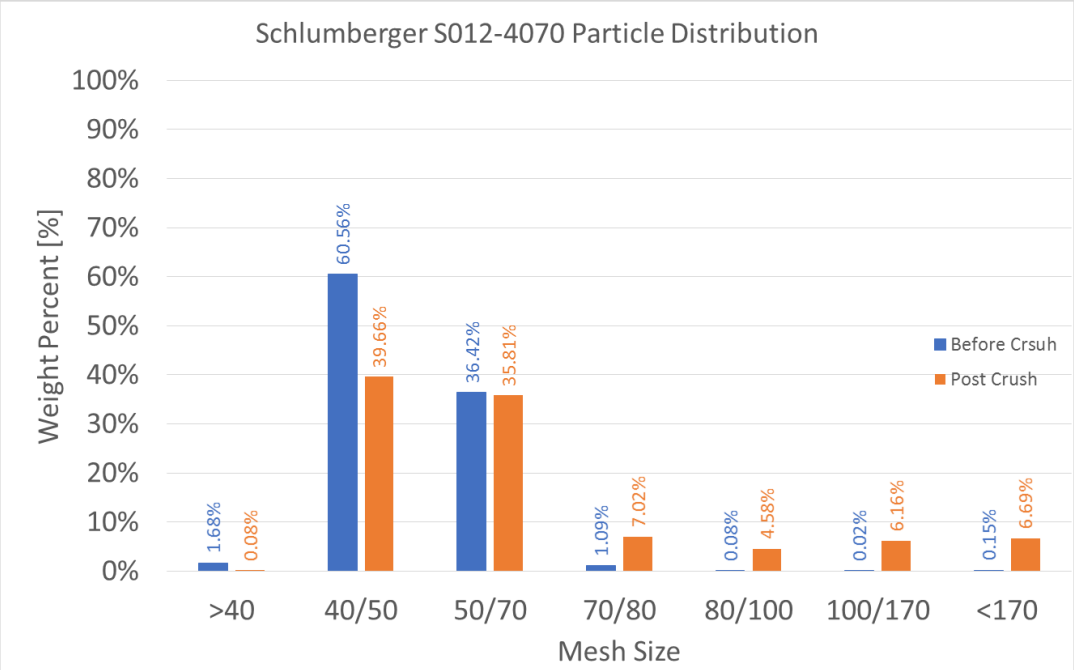

Figure 3.16 Size distribution of Schlumberger SO12 4070 Mesh

3.1.2.3 Fracture Conductivity

The 40/70 mesh sand was the second most conductive proppant tested. As proppant size decreases, so does the fracture conductivity. This result was very much expected and again, the proppants were grouped together when plotted against each other's. Sphericity and roundness, or lack thereof, is the likely explanation for the large deviation in fracture conductivity curve trends when comparing Schlumberger SO12 to the other two proppants of the same size. A tight proppant pack that has considerably lower fracture permeability is the result of triangular shaped proppants, as seen in Figure 3.13.

While Schlumberger Brown had the highest initial conductivity, it also experienced a slightly higher percentage of crushing when compared to Schlumberger

White proppant. The ability for Schlumberger White proppant to not deform as much at high closure stresses is evident in the decline of its fracture conductivity curve. At 3000 psi closure stress, Schlumberger Brown and White have essentially the same fracture conductivity and the curves overlap until 6000 psi is reached. When comparing the slopes of the curves, it can be interpreted that Schlumberger Brown proppant is experiencing crushing and producing fine particles that are reducing permeability more severely per closure stress interval. Thus, a more negative slope is observed with the Schlumberger Brown proppant and has a larger range of conductivity's calculated between 1000 and 6000 psi closure stress. Schlumberger SO12 experienced a nearly twofold crushing percentage when compared to the other proppants. This can be identified by the wide gap in conductivity curves, observed in Figure 3.16.

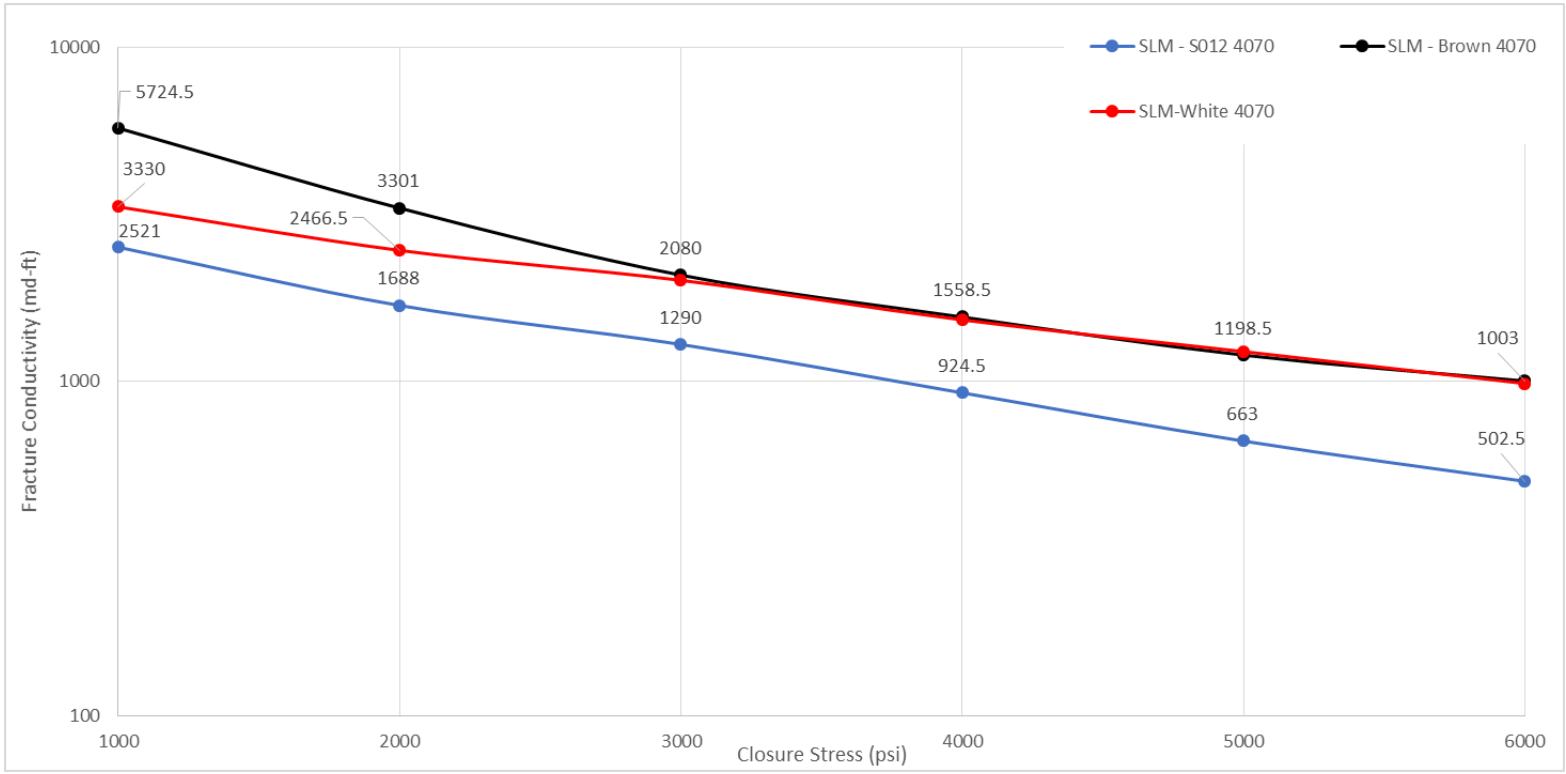

Figure 3.17 Fracture conductivity results of 4070 Mesh sand proppants tested

3.1.3 100 Mesh

Proppant Number	Proppant Type	Proppant Name	Number of Tests Completed
2	100 Mesh Sand	HAL - Local	2
6		HAL - Prem. White North	2
7		SLM - Brown	2

Table 3.4 100 Mesh Sand Testing Matrix

3.1.3.1 Proppant Geometry

The proppant geometry for the three proppant tested were all very different. Halliburton Silica Local 100 Mesh had the largest deviation from what an optimum particle sphericity and roundness is defined as, as seen in Figure 3.18. Some particles were very elongated and almost rectangular in shape, while others mimicked a more triangular shape. The particles that had a spherical shape tended to be more round than those of another shape. Halliburton Premium White Northern was the most consistently spherical and round of the three proppant that are being compared. Schlumberger Brown 100 Mesh was far more spherical and round than the Halliburton Silica, but not nearly as consistent as the Halliburton Premium White Northern. Few of its particles had extremely jagged edges

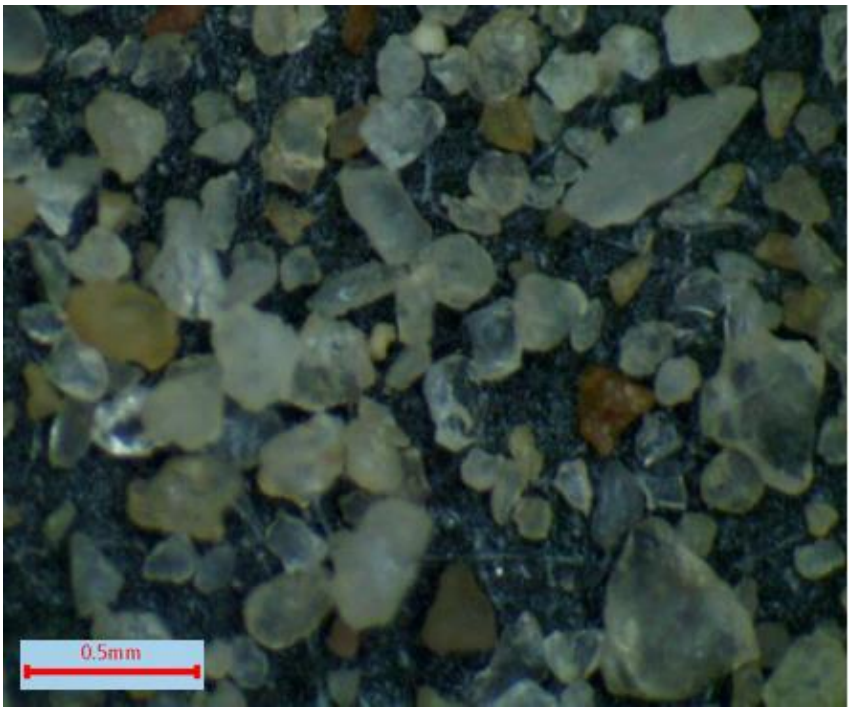

Figure 3.18 Magnification of Halliburton Local 100 Mesh

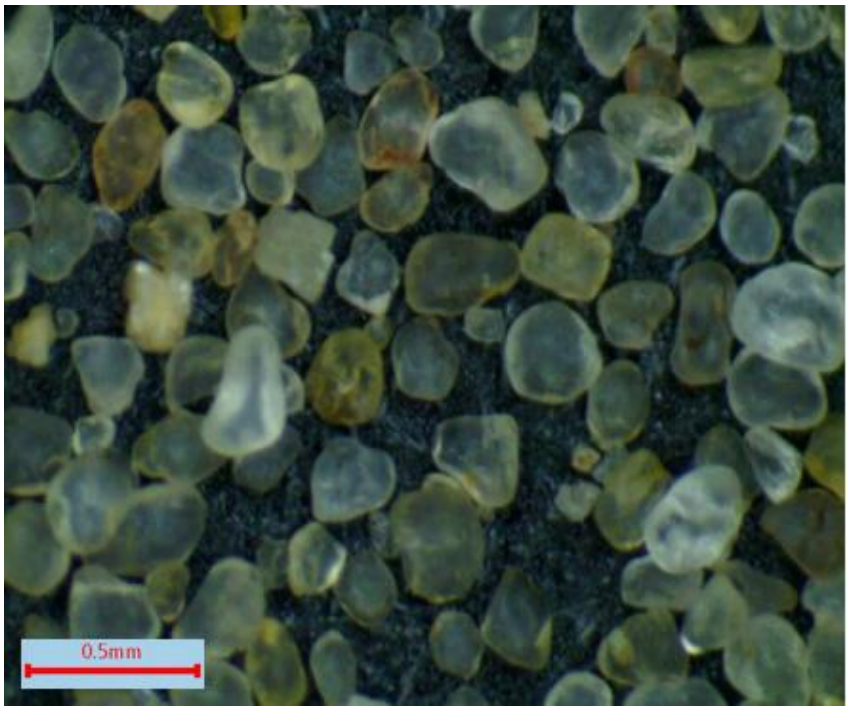

Figure 3.19 Magnification of Halliburton Premium White Northern 100 Mesh

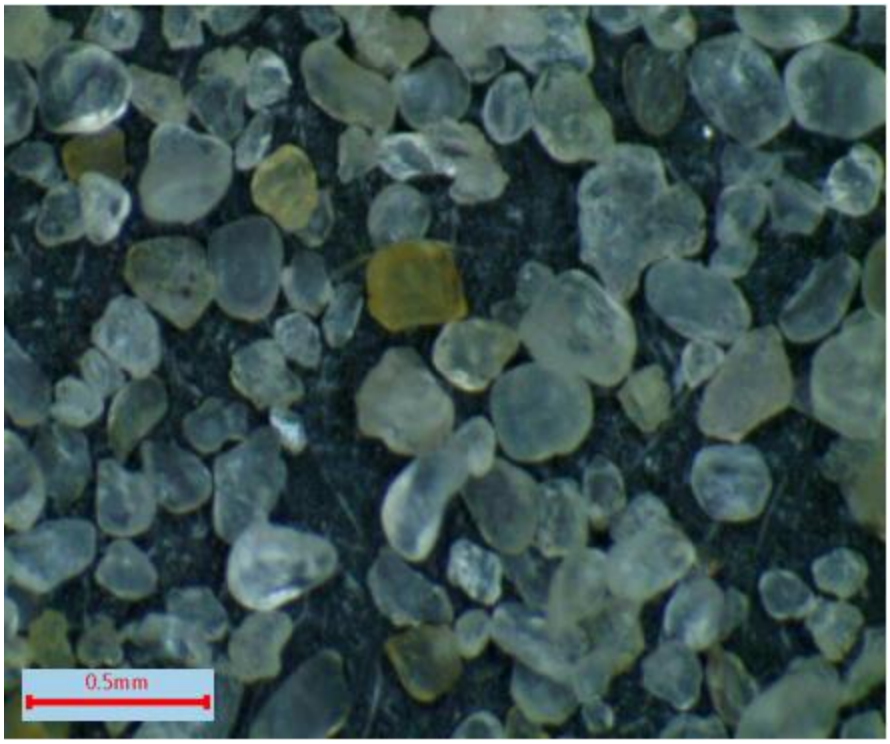

Figure 3.20 Magnification of Schlumberger Brown 100 Mesh

3.1.3.2 Proppant Distribution and Crushing

A 100 mesh proppant distribution is different than its 30/50 or 40/70 counterparts because it is not defined between a ranges of mesh sizes, but rather just one size. Albeit, most proppant particles should be close in size to a 100 mesh, this is not always true. Halliburton 100 Mesh Local proppant has a large size distribution when a sieve analysis is conducted, such that there is a substantial percentage of proppant mass that is larger than 40 mesh. Figure 3.21 provides a visual confirmation. Halliburton Premium White Northern and Schlumberger Brown had a much tighter range of particle size, where a majority of particles were between 50 and 170 mesh.

Halliburton 100 Mesh Local had a crushing percentage of approximately 11%. The larger particles experience crushing and add to the size distribution of the smaller ones. This is evident in the percent increase of the proppant ranging from 80 mesh, to that smaller than 170 mesh. Halliburton Premium White Northern experienced the least amount of crushing at 9%. While not a severe amount, Schlumberger Brown experienced the most crushing at 12%. A proppant that has a larger percent of crushing will likely experience worse fracture conductivity results.

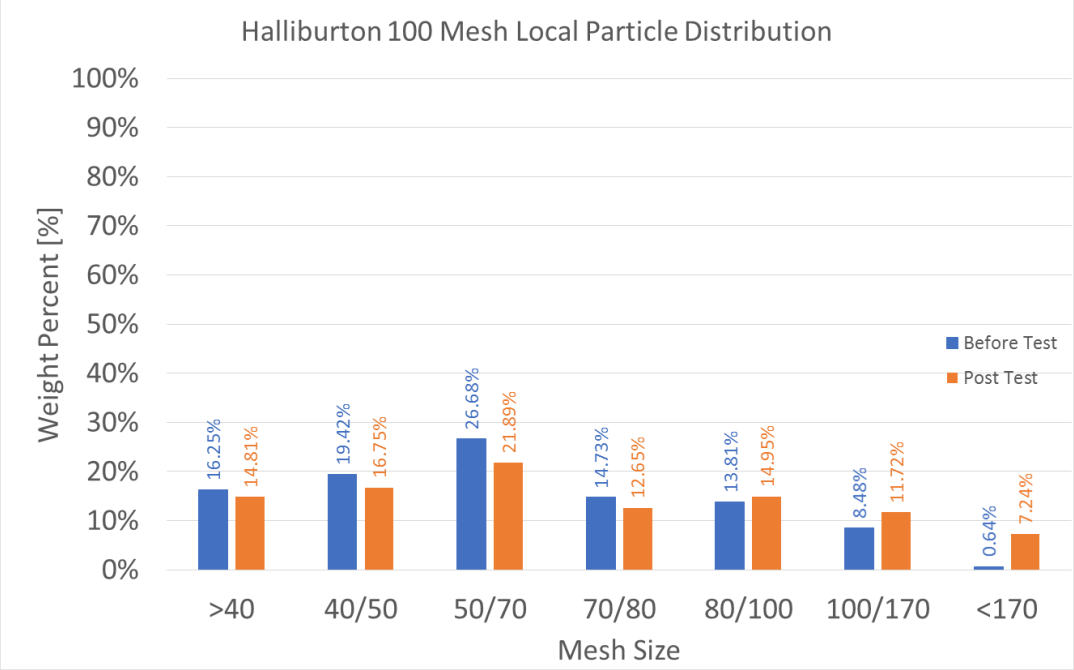

Figure 3.21 Size distribution of Halliburton Local 100 Mesh

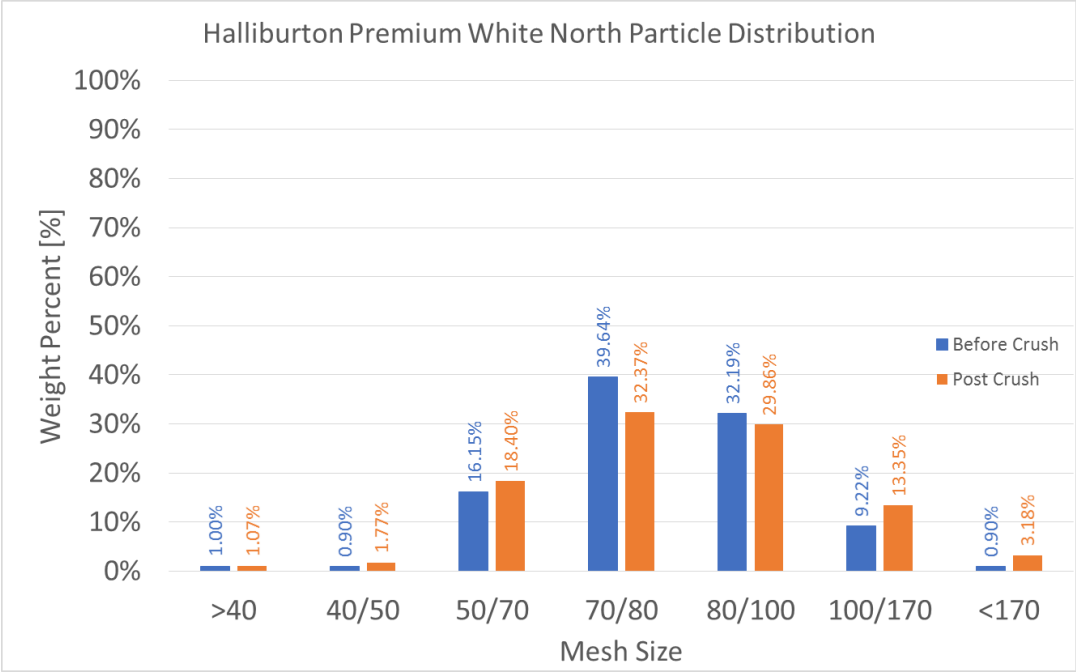

Figure 3.22 Size distribution of Halliburton Premium Northern 100 Mesh

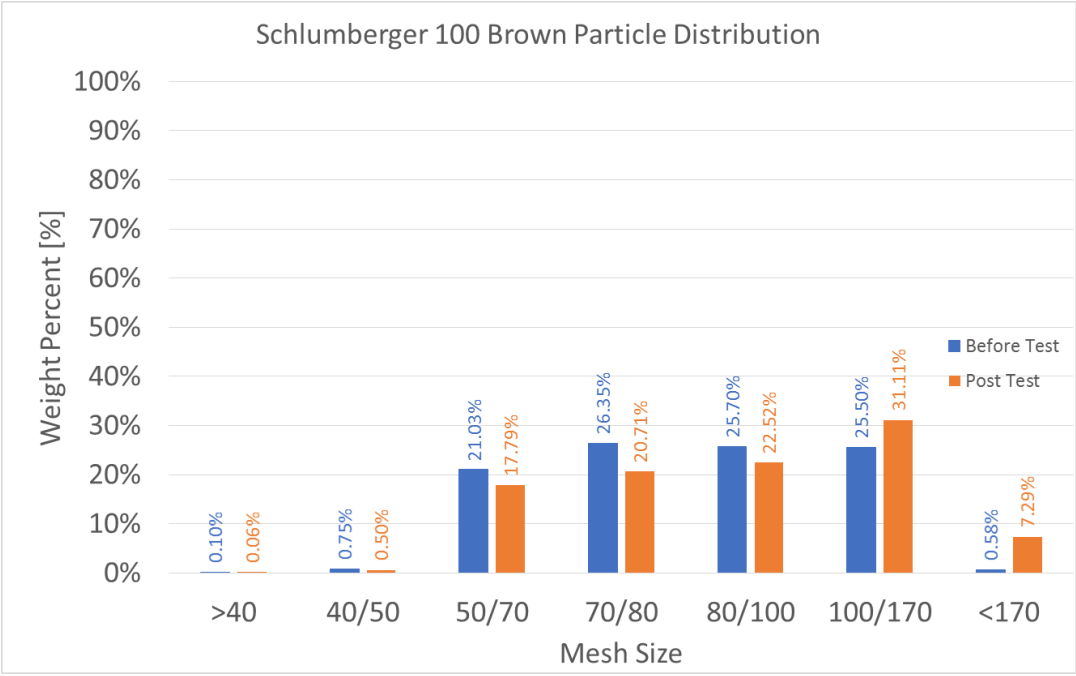

Figure 3.23 Size distribution of Schlumberger Brown 100 Mesh

3.1.3.3 Fracture Conductivity

As a whole, the 100 mesh sand was the least conductive proppant size amongst all sand proppants tested. The smaller sized particles are not able to maintain as permeable of a proppant pack as the 30/50 or 40/70 mesh sizes. This has a direct correlation to the resulting fracture conductivity which is the product of the fracture width and the proppant pack permeability. Figure 3.3 presents the 100 mesh proppant grouping as the least conductive proppant size, being that the curves of all proppants of said mesh size are at the bottom of the spectrum.

The Halliburton 100 Mesh Local proppant had the highest initial fracture conductivity. This was likely due to the large proppant size, being that a well-defined proppant size range was not observed. However, large particles experience more crushing than those that are smaller, leading to the creation of fines, and reducing conductivity at a greater rate. As well, the lack of sphericity and roundness of the proppant will also decrease the conductivity.

In opposition, Halliburton Premium White Northern had a lower initial conductivity because particle sizes were closer to a true 100 mesh. The sphericity and roundness of the proppant was very consistent, which helped to maintain conductivity at high closure stresses. The conductivity curves of the two cross at 4000 psi. This is indicative of the Halliburton Premium White Northern experiencing less crushing and ultimately resulting in a higher conductivity at 6000 psi.

The Schlumberger 100 Mesh Brown had the smallest size distribution amongst all 100 mesh proppants tested, with 26% of proppant between 100 and 170 mesh, prior

to any crushing occurring. This is evident in that it had a slightly lower initial fracture conductivity when compared to Halliburton Premium White Northern. It also did not have nearly as consistent sphericity or roundness as Halliburton Premium White Northern and experienced the highest crushing percentage amongst the three 100 mesh sand proppants discussed. These factors played a role in Schlumberger 100 Mesh Brown providing the worst fracture conductivity results for this mesh size.

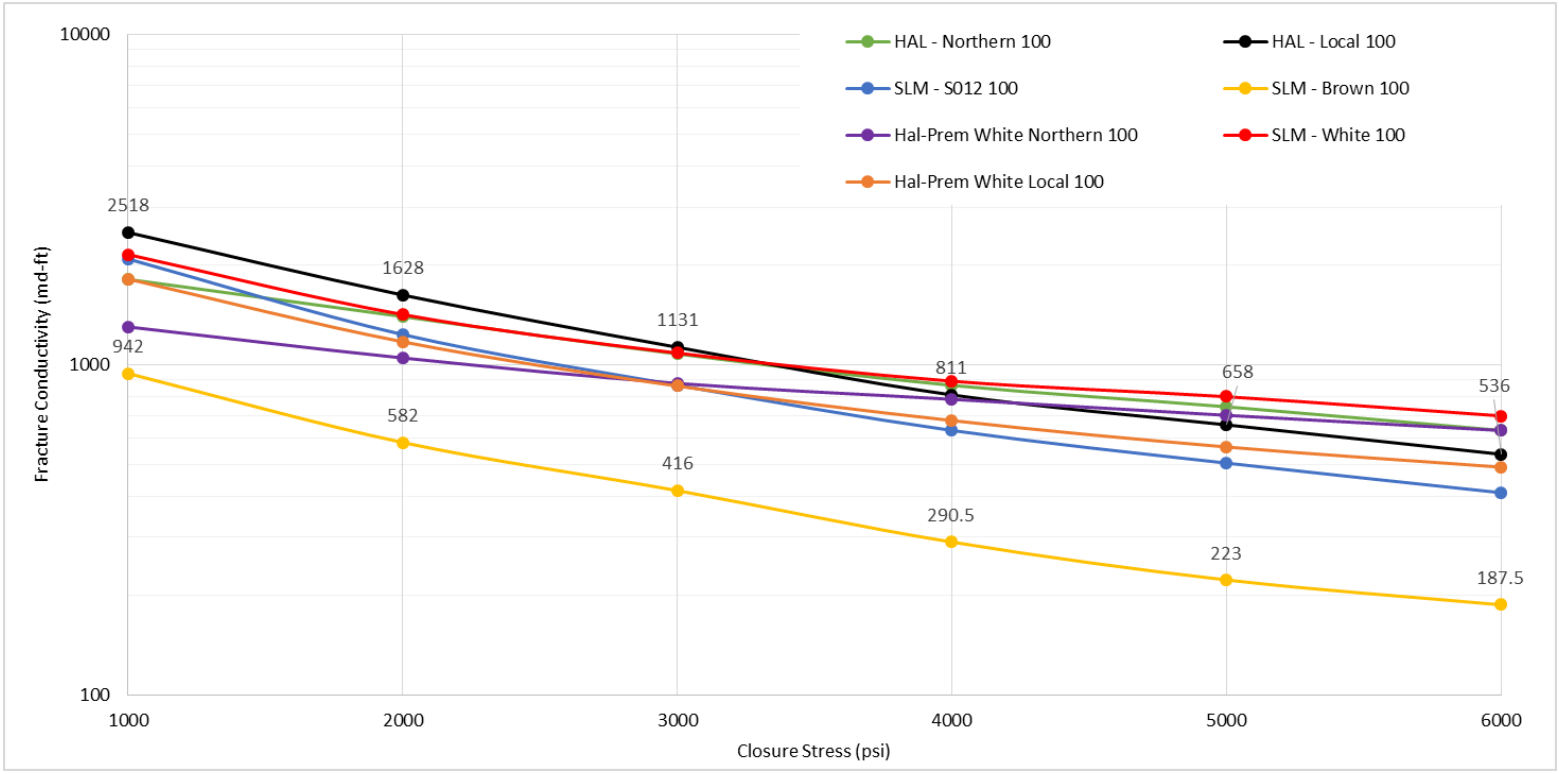

Figure 3.24 Fracture conductivity results of 100 Mesh sand proppants tested

3.2 Taconite

The taconite that was tested is from four different mines. Two mesh sizes, 40/70 and 100 mesh were tested. As seen in Figure 3.25, a wide range of results were found regarding fracture conductivity. The following section will be used to present the results and bring insight to the variables that effect the conductivity.

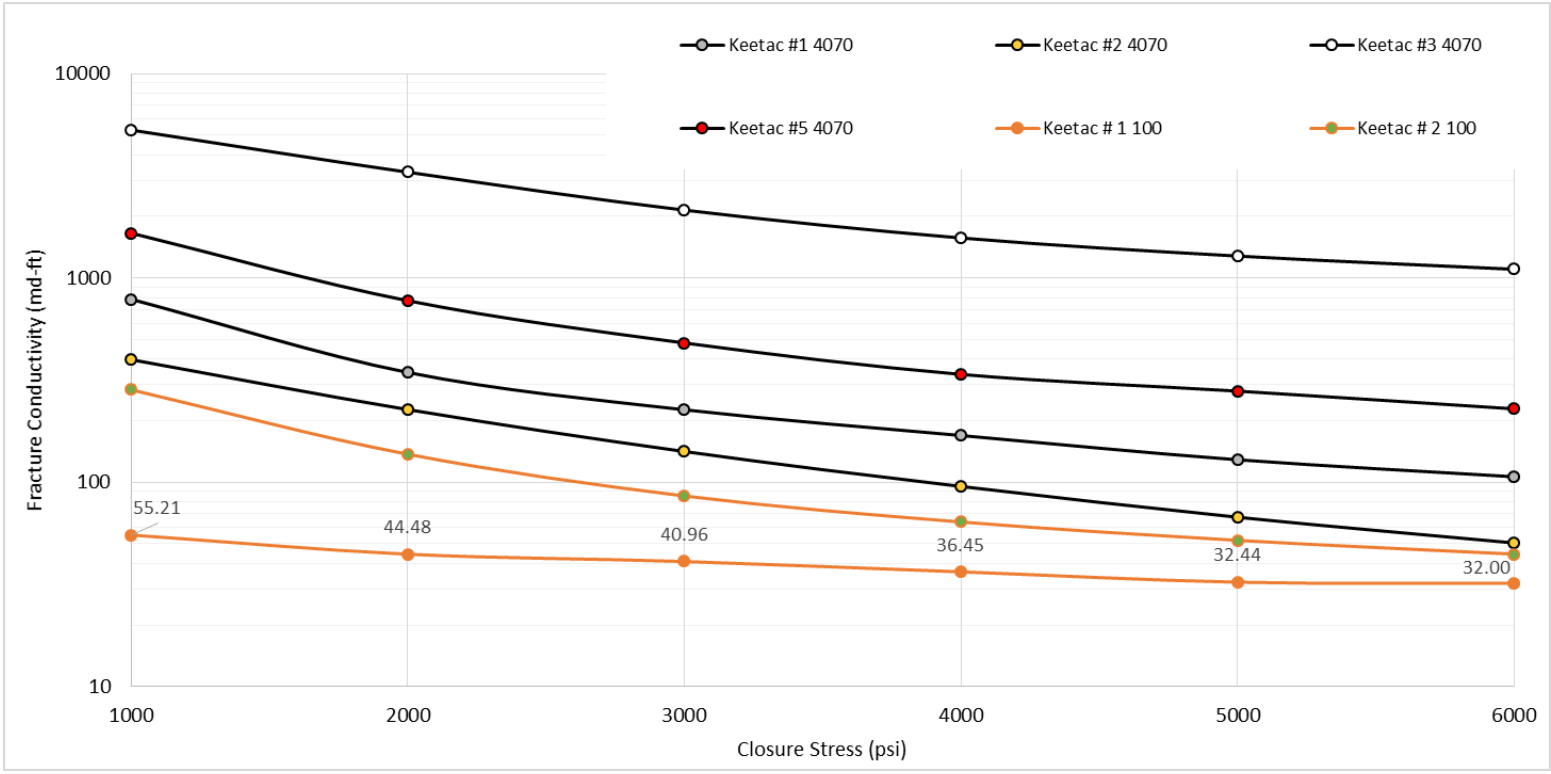

Figure 3.25 Fracture conductivity results of all Keetac Taconite sample proppants tested

3.2.1 40/70 Mesh

Proppant Number	Proppant Type	Proppant Name	Number of Tests Completed
16	40/70 Mesh Tactonite	Keetac #2	2
17		Keetac #3	2
18		Keetac #5	2

Table 3.5 40/70 Mesh Taconite Testing Matrix

3.2.1.1 Proppant Geometry

A wide variety of 20/40 mesh taconite geometry was observed at the microscopic level. The proppant that was provided from Keetac Sample #2 and Keetac Sample #3 are fairly similar in terms of sphericity and roundness. There is a variation amongst particles in which some are more spherical and round than others and as a whole are not as consistent as sand proppant. Keetac Sample #5 proppant is far less spherical and has many more jagged edges.

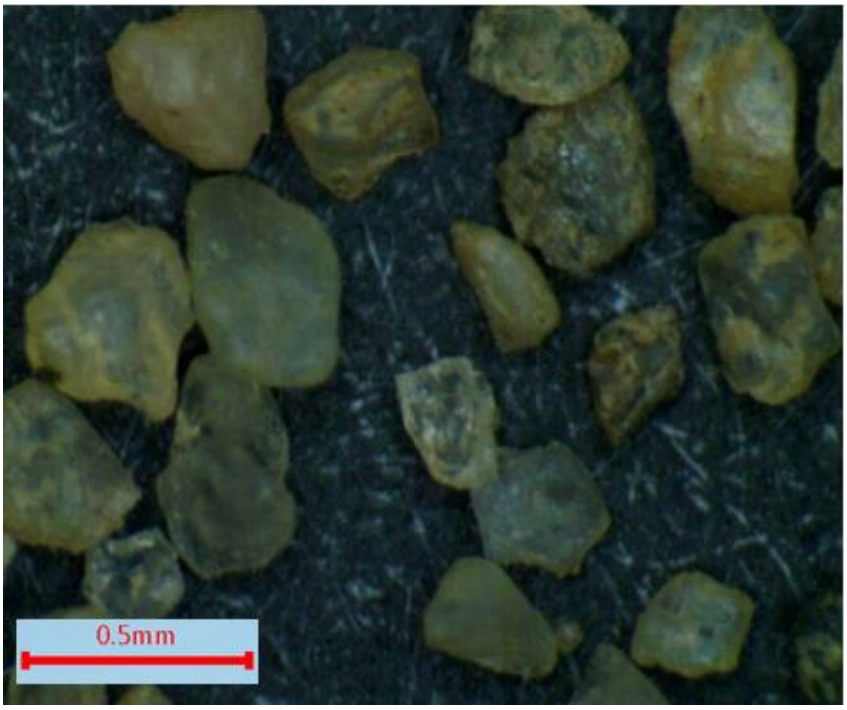

Figure 3.26 Magnification of Keetac Sample #3 4070 Mesh

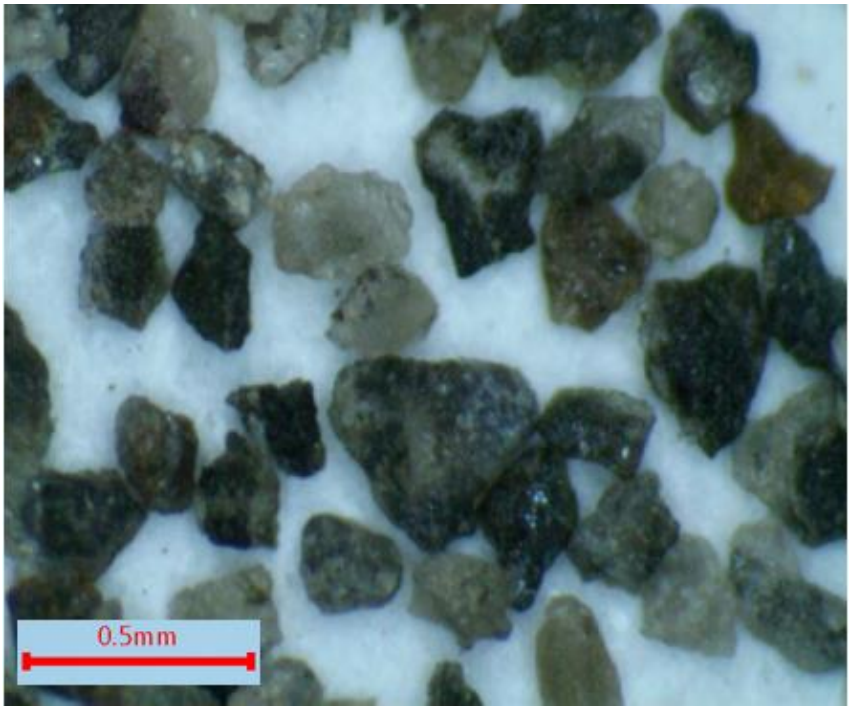

Figure 3.27 Magnification of Keetac Sample #5 4070 Mesh

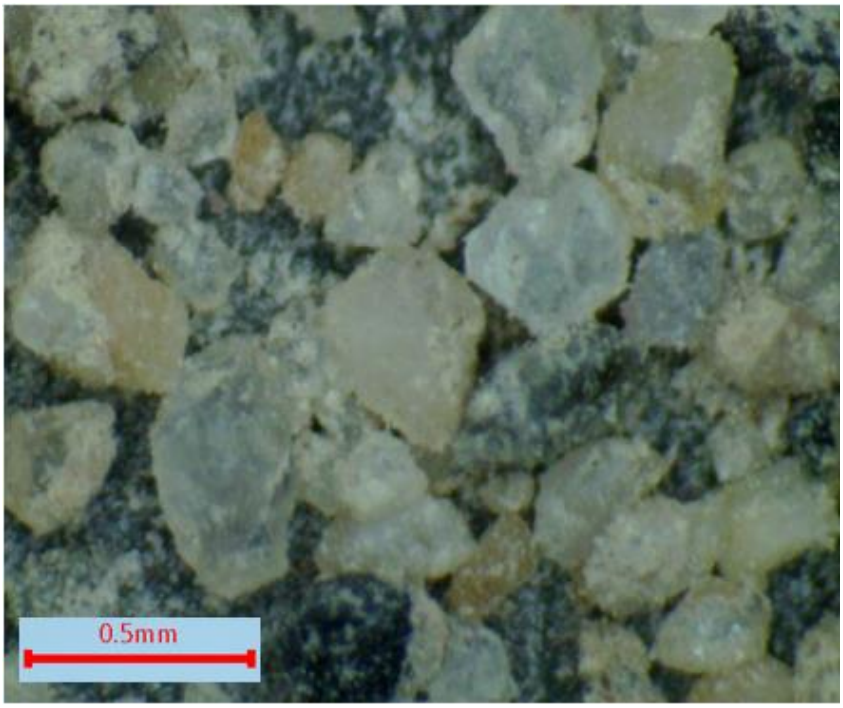

Figure 3.28 Magnification of Keetac Sample #2 4070 Mesh

3.2.1.2 Proppant Distribution and Crushing

The proppant distribution of this 40/70 taconite mesh requires that 90% of proppant should fall through the 40 mesh and be withheld by the 70 mesh. Proppant from Keetac Sample #3 and Keetac Sample # 5 fit this criterion, however the proppant from Keetac Sample # 2 only has 70% of mass between 40 and 70 mesh prior to crushing. This lends to the idea that smaller particles will result in lower fracture conductivity. Keetac Sample #2 saw the least amount of crushing at only 15 %, however this could be due to there being fewer large particles to begin with. Keetac Sample's #3 and #5 both had a crushing of 23%, increasing the number of small particles that can reduce conductivity.

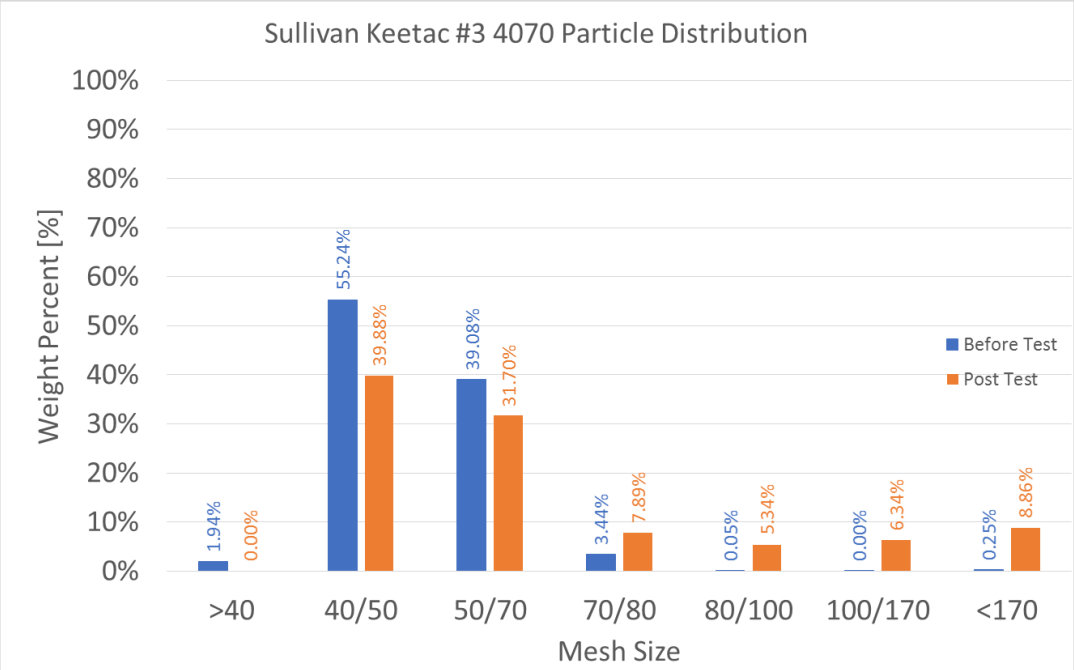

Figure 3.29 Size distribution of Keetac Sample #3 4070 Mesh

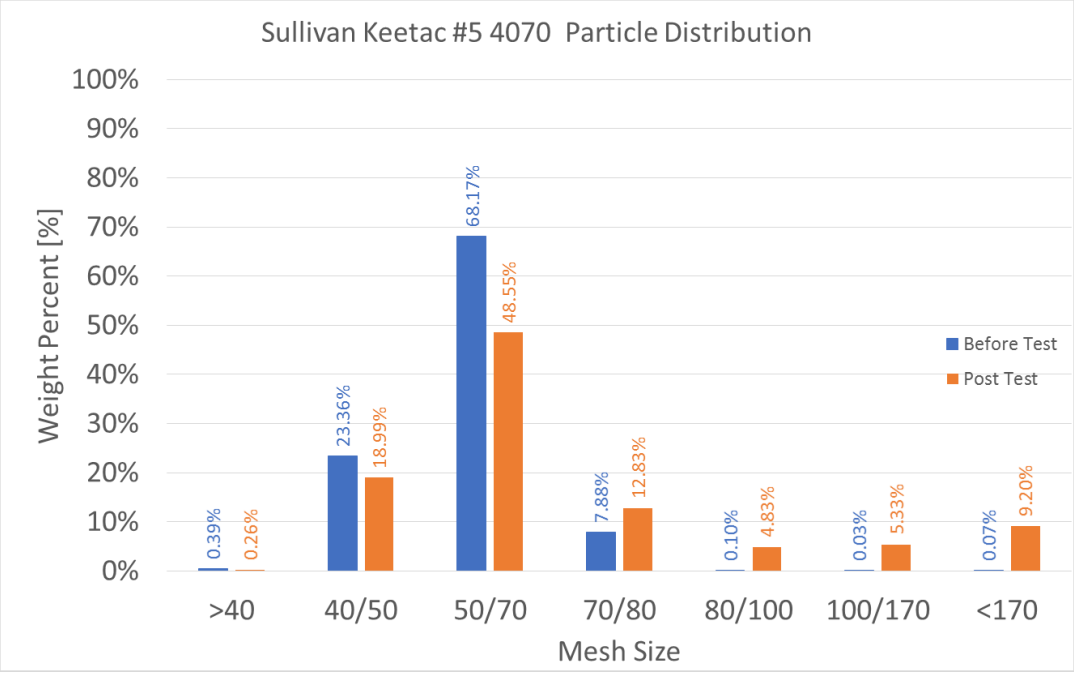

Figure 3.30 Size distribution of Keetac Sample #5 4070 Mesh

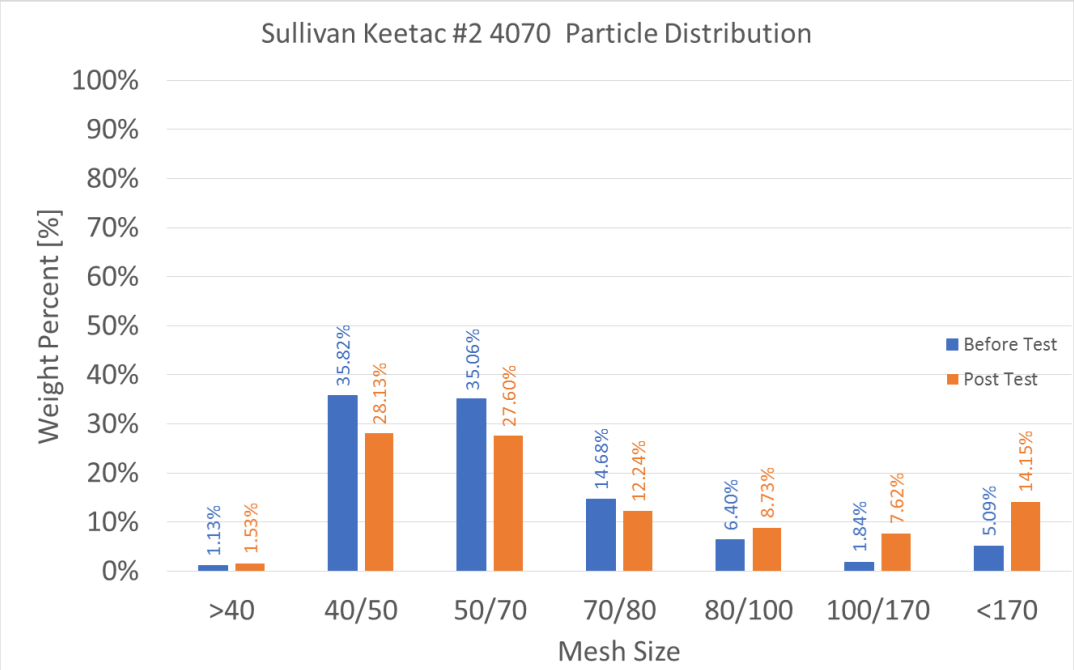

Figure 3.31 Size distribution of Keetac Sample #2 4070 Mesh

3.2.1.3 Fracture Conductivity

The fracture conductivity of the taconite proppant had a large variation in results. Figure 3.33 shows the results of the four taconite proppants tested and compares them to sand proppants of the same size. Figure 3.32 provides a closer look at only the conductivity of 40/70 mesh taconite. All four proppants follow a general declining trend and there is no over-lapping of conductivity curves. If two proppants were close in conductivity values and a crossing of the curves occurred, this would provide insight as to one proppant suffering crushing much more severally than the other.

The Keetac Sample #3 had a substantially higher fracture conductivity than its peers. This can be attributed to a proppant distribution that is true to a 40/70 mesh, limited crushing, and a more spherically shaped proppant than its counterparts. Keetac

Sample #5 had a threefold reduction in conductivity when compared to Keetac Sample #3 at the initial 1000 psi closure stress. This sample had a very different shape than its counterpart, with many particles having an almost triangular shape, with sharp edges. As a result, when closure stress is applied, the particles are able to mesh together, rather than supporting one another. This is a possible explanation for the lower conductivity experienced. However, it still provided reasonable conductivity results and if it had a size distribution that was on the larger end of the 40/70 mesh size spectrum, it could possibly provide results similar to Keetac Sample #3.

Keetac Sample # 2 provided extremely poor conductivity results. While the shape is not much different than that of Keetac Sample #3, a closer look at the proppant reveals extremely fine particles that seem to have stuck to the surface of the proppant, as well as a much smaller size distribution. Keetac Sample # 1, shown in Figure B.6 of the Appendix B, also has similar fine particles on the surface, supporting similar results. These fine particles essentially act as crushed proppant and due to fine migration, will collect between the pore spaces of the proppant, reducing permeability of the proppant pack and thus fracture conductivity.

Figure 3.33 displays the conductivity curves of the 40/70 mesh taconite samples, as well as the 40/70 mesh sands. Keetac Sample #3 provides fracture conductivity results that are comparable or better than the conventional sands of the same size. The other three samples did not perform well when compared to the tested sand proppants.

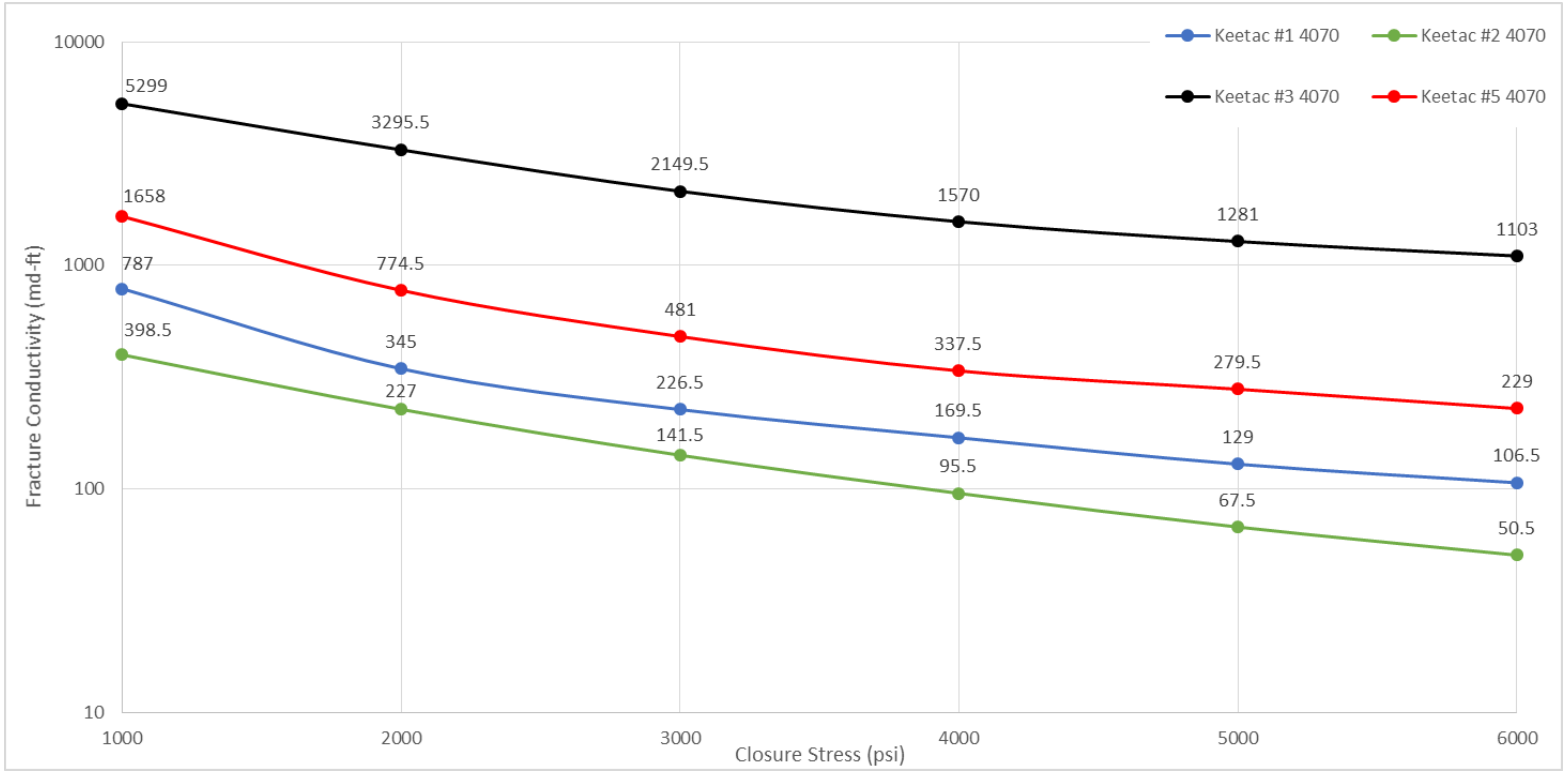

Figure 3.32 Fracture conductivity results of all 4070 Mesh Keetac Taconite samples

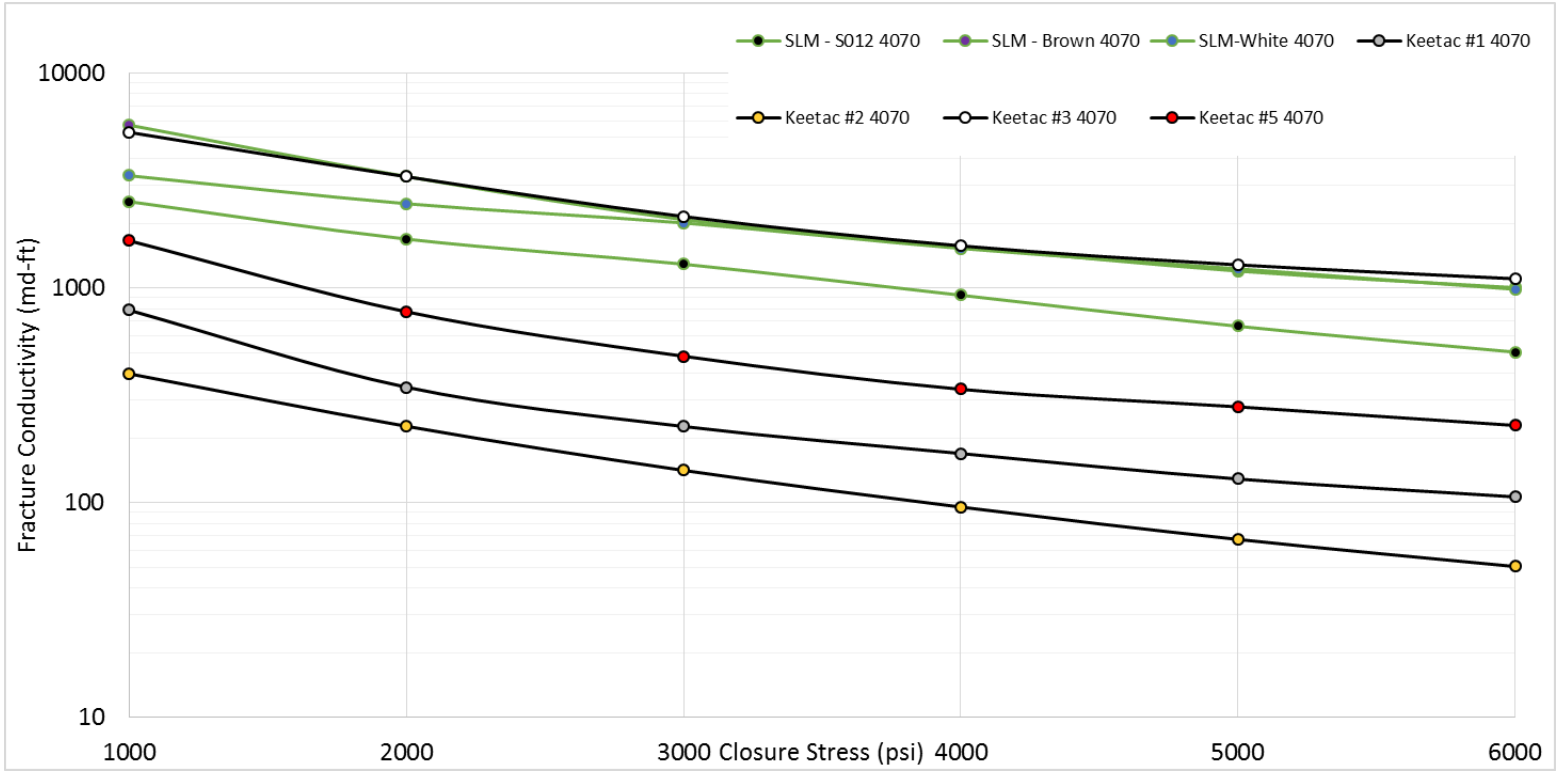

Figure 3.33 Fracture conductivity of 4070 Mesh Keetac Taconite samples compared to 4070 Mesh conventional sand

3.2.2 100 Mesh

Proppant Number	Proppant Type	Proppant Name	Number of Tests Completed
19	100 Mesh Taconite	Keetac #1	2
20		Keetac #2	2

Table 3.6 100 Mesh Taconite Testing Matrix

3.2.2.1 Proppant Geometry

The two geometries of the 100-mesh taconite proppant are amongst the most difficult to define of all proppants tested. The Keetac Sample #2 proppant particles have fairly rounded edges but are not as spherical as a majority of a sand proppant of the same size. The larger particles of the Keetac Sample #1 that were able to be identified, had decent roundness, but were not found to be very spherical. The particles that are very small appear to not be very spherical or round in nature. When comparing proppant shape to a Krumbein and Sloss chart, Keetac Sample #2 100 mesh proppant should provide better fracture conductivity results than Keetac Sample #1 100 mesh.

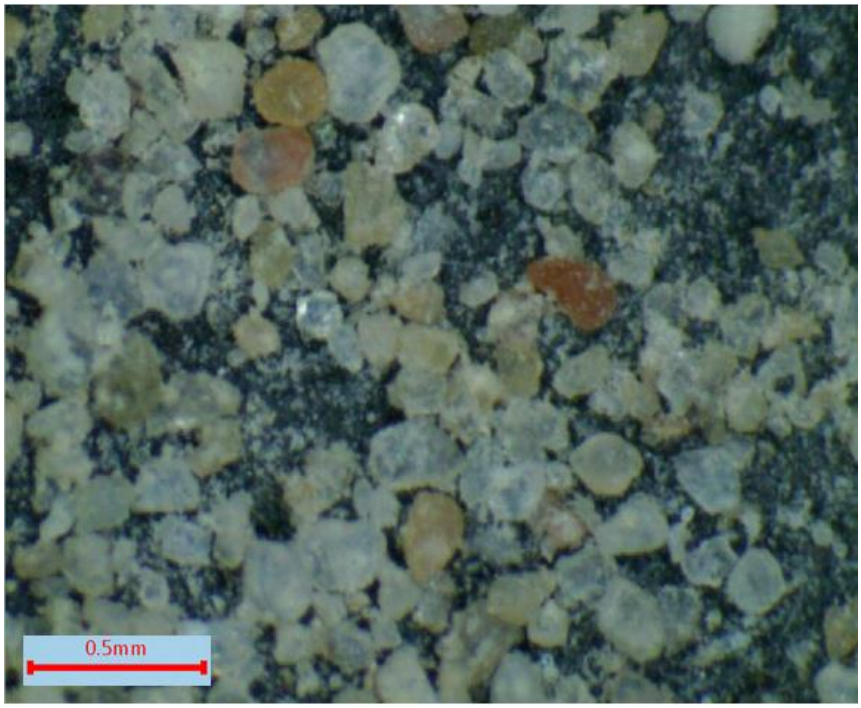

Figure 3.34 Magnification of Keetac Sample #2 100 Mesh

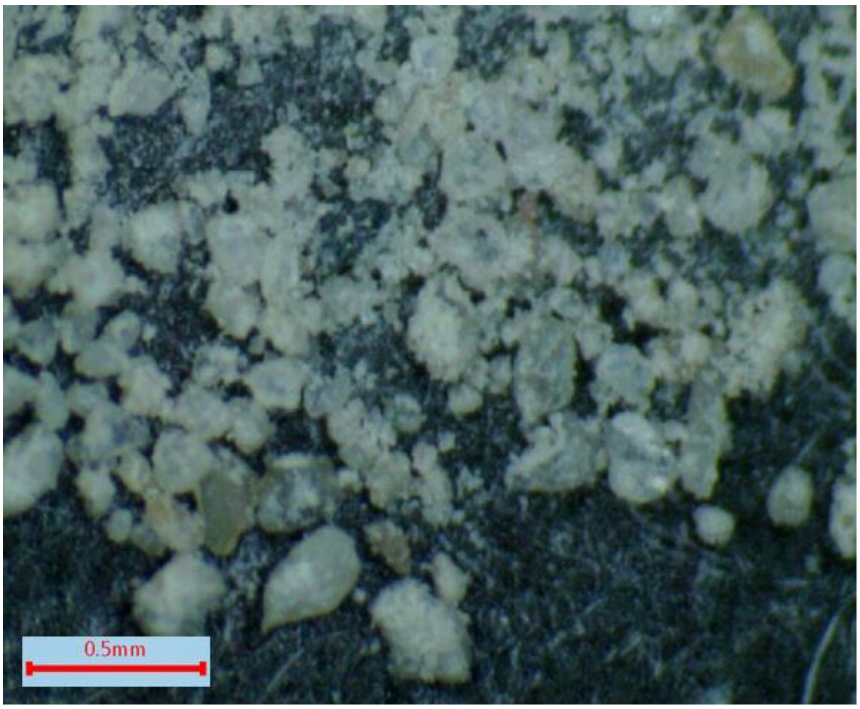

Figure 3.35 Magnification of Keetac Sample #1 100 Mesh

3.2.2.2 Proppant Distribution and Crushing

As has been previously discussed, a 100-mesh proppant is not defined by an upper and lower limit mesh size. As a result, an inconsistent variation in proppant distribution can be found amongst many different proppants that are characterized as being 100 mesh. This was evident with the size distribution of 100 mesh sands and is also experienced with both 100 mesh taconite samples. Keetac Sample #2 provided a particle size distribution in which most of the distribution was closer to 100 mesh than the Keetac Sample #1. This is because it only had 8% of proppant that was smaller than 170 mesh, while Keetac Sample #2 had upwards of 28%. Based on theory alone, significantly smaller particles will provide worse conductivity, prior to any crushing occurring.

The larger size distribution of the Keetac Sample #2 resulted in a larger percentage of proppant crushing when compared to Keetac Sample #1. This is an expected outcome as very small particles, such as those that make up Keetac Sample #1, cannot crush much more than their original size. Keetac Sample #2 suffered from 14% crushing compared to just 6% of its counterpart. A proppant that undergoes a larger percentage of crushing will reflect this in the fracture conductivity curve.

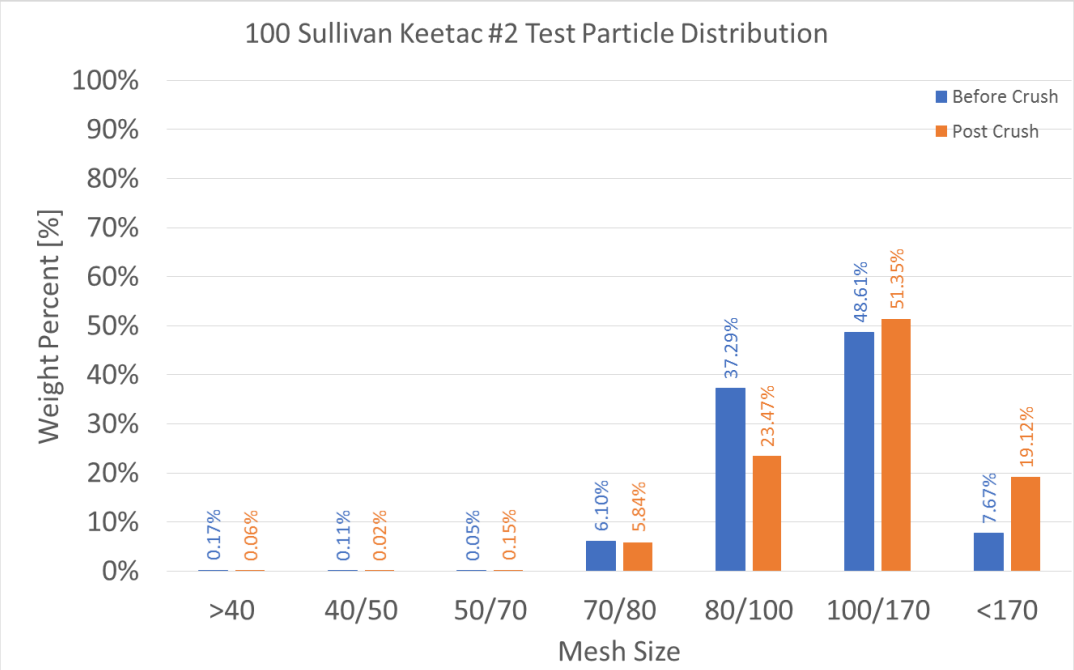

Figure 3.36 Size distribution of Keetac Sample #2 100 Mesh

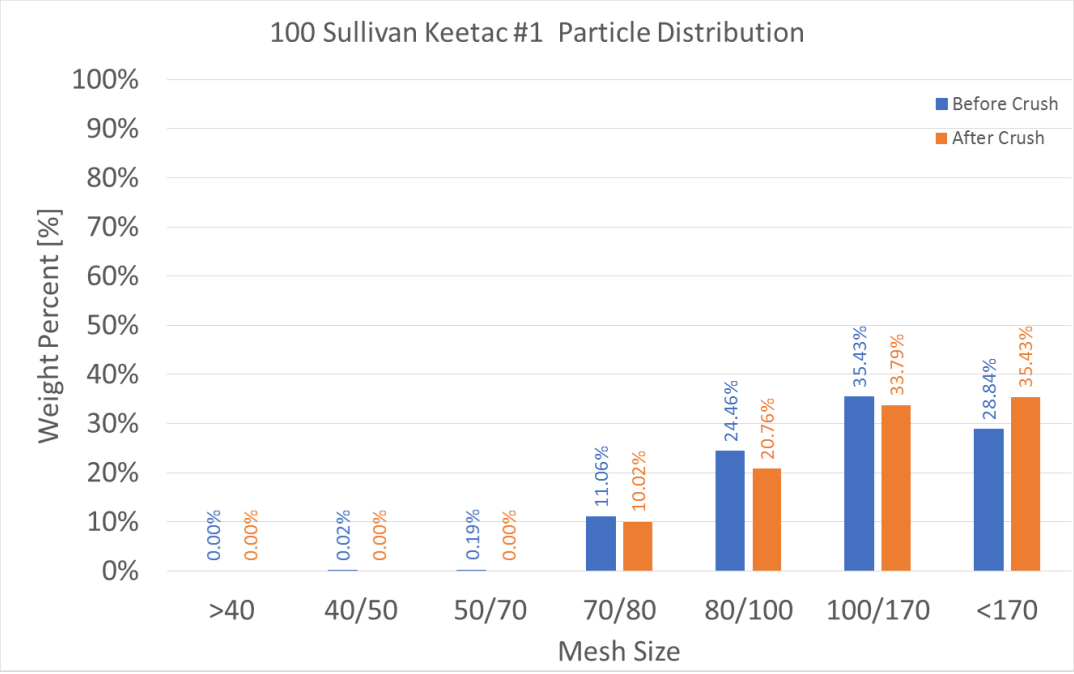

Figure 3.37 Size distribution of Keetac Sample #1 100 Mesh

3.2.2.3 Fracture Conductivity

The 100-mesh taconite proppant did not provide good results for fracture conductivity as both samples had an initial conductivity of less than 300 md-ft at 1000 psi closure stress. As closure stress increased, the fracture conductivity declined to extremely low values of 45 and 32 md-ft. respectively, at the final closure stress of 6000 psi. The extremely small proppant size distribution, as well as the irregularities from a round, spherical shape is what causes such low conductivity.

Size distribution plays a vital role in the fracture conductivity of this novel proppant. When testing the 40/70 mesh size taconite proppants, Keetac Sample #1 had higher fracture conductivity values at each respective closure stress when compared to Keetac Sample #2. This is due to having a larger percentage of particles be in the 40/70 mesh range. In contrast, for the 100 mesh samples, Keetac Sample #2 had a larger size distribution and thus had higher conductivity values when compared to Keetac Sample #1.

Figure 3.39 displays the fracture conductivity curves for only the two 100 mesh taconite proppants tested. Keetac #2 has a much steeper decline in conductivity when compared to the Keetac Sample #1. A higher percentage of proppant crushing for Keetac Sample #2 is likely the cause of this trend. Both proppants had the same fine particles, as seen with the 40/70 sized proppant of the same sample that are seemingly stuck to the particle surface. When crushing occurs, the movement of these fine particles will reduce permeability considerably. Keetac Sample #1 proppant pack permeability was reduced so much so, that it resulted in an impermeable wafer, as seen in Figure 3.38. Thus, the

inability for fluids to flow through the porous media will have devastating effects on fracture conductivity.

When comparing the Keetac 100 mesh samples to conventional sand proppants of the same size, the taconite provides far worse conductivity results. Figure 3.40 shows the comparison of the two types of different proppants. All taconite 100 mesh conductivity curves are far below any of the conventional sand proppants of the same size. However, Keetac Sample #3, which had comparable conductivity values to conventional sand at 40/70 mesh size, was unable to be tested due to the lack of necessary volume required to run a test. This proppant a mesh size of 100 may provide results comparable to conventional sand.

Figure 3.38 100 Mesh Keetac Sample #1 after conducitivty test

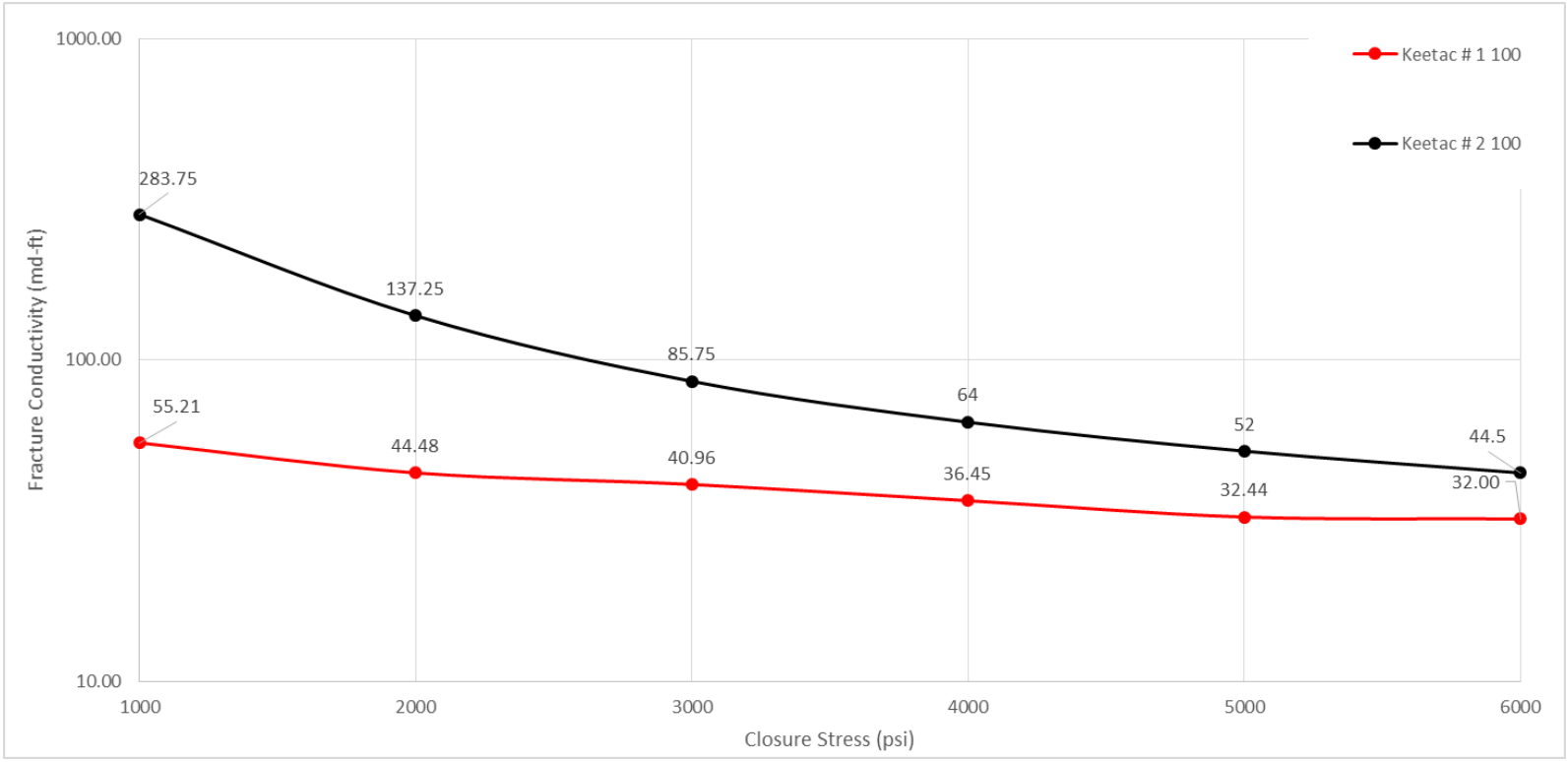

Figure 3.39 Fracture conductivity results of all 100 Mesh Keetac Taconite sample

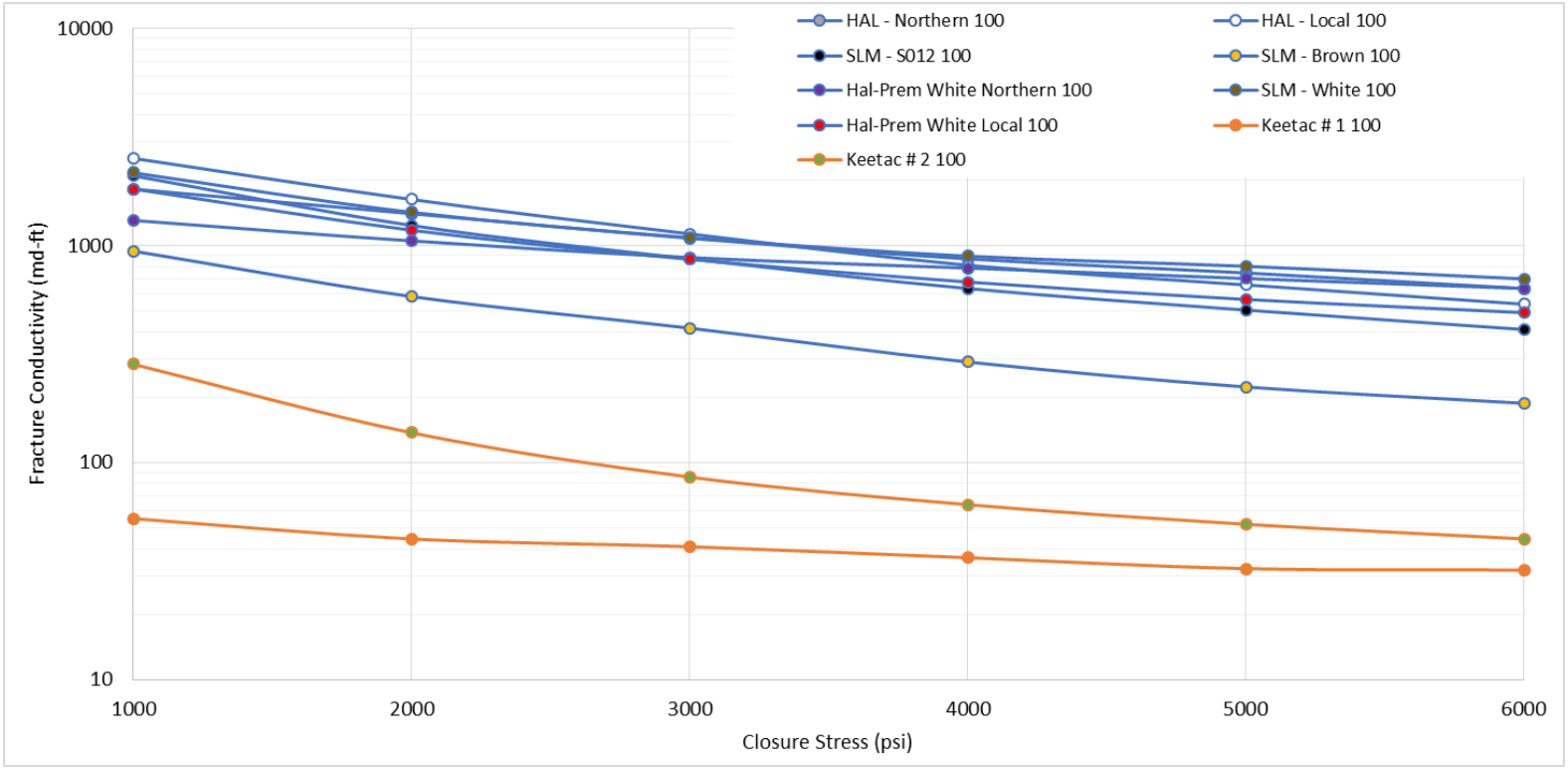

Figure 3.40 Fracture conductivity of 100 Mesh Keetac Taconite samples compared to 100 Mesh conventional sand

4. CONCLUSION AND RECOMMENDATIONS

4.1 Conclusions

This study was conducted in order to evaluate the fracture conductivity behavior of 20 different proppants. These proppants were conventional sand and taconite, which is characterized as a novel proppant. Tests were conducted in a multitude of different mesh sizes and the results were compared. All testing procedures followed the API RP 61 guidelines for testing a proppant pack under short term conditions.

All sand proppants tested provided viable options for fracture conductivity and a closer look at a cost benefit analysis would provide quality insight as to which specific proppant of a given size should be used for a given fracture treatment. The results showed that proppant size is the variable that has the most impact in regards to fracture conductivity. As a whole, when comparing a proppant type, the larger mesh size had higher conductivity than that of a smaller mesh size. As well, those proppants which displayed a more spherical and round shape, consistently had higher conductivity than those that did not.

Local proppant provided superior results at the low closure stresses of 1000-3000 psi for a 100 mesh sand proppant when compared to a brown or white sand of the same size. It also only had slightly worse fracture conductivity results at higher closure stresses when compared to that same proppant. However, this is deceiving as it had a very large size distribution. Due to the lack of sphericity and roundness, if the local sand had a comparable size distribution to the brown or white sand proppants, it would provide far worse conductivity results.

The testing of taconite as a novel proppant and one that could be a possible substitute for conventional sand proppants was not definitive. It can be said that in a quality condition, taconite can indeed provide reasonable fracture conductivity and thus, possibly be used as an alternative. However, taconite being a novel proppant, is far less consistent in sphericity and roundness. As well, the purity of the proppant may come into question when extremely fine particles are found to be sticking to the proppant surface, thus reducing the permeability by a substantial amount.

4.2 Recommendations

It is not believed that local sand proppant has potential to outperform any manufactured proppant or brown or white sand, however, this is not to say that it is not a capable proppant. To gain a true insight into its performance, it is recommended that testing of local proppants be conducted at 30/50 and 40/70 mesh size because these size distributions have an upper and lower limit. Following the 90% rule for proppant size distribution, results should show that local proppant will provide consistently lower conductivity results. However, the resulting conductivity is often enough for the production of shale plays, at a much cheaper cost.

It is believed that taconite has potential as a novel proppant. Due to the lack of volume, Keetac Samples #3 and #5 were unable to be tested at the 100 mesh size. It would be interesting to see if an impermeable wafer would form due to high closure stresses with these proppants as they did not have the fine particles that stuck to the surface of the proppant, as seen with their 40/70 mesh size.

As well, in regards to the two samples that had fine particles attached to the surface of the proppant, a turbidity test is recommended. Turbidity is the measure of suspended particles in water. This test provides insight as to the purity of a proppant and can reveal any dirt or silt that may be attached to each particle. These particles act as fines in the proppant pack pores, reducing permeability. All commercial proppants are within the threshold of an acceptable turbidity tests before being sold and as such, proppant purity was never an issue with any of the conventional sand proppants. This testing method can be found in API RP 19C.

REFERENCES

Alramahi, B., & Sundberg, M. I. (2012, January 1). Proppant Embedment And Conductivity of Hydraulic Fractures In Shales. American Rock Mechanics Association.

American Petroleum Institute. Recommended Practices for Evaluating Short Term Proppant Pack Conductivity. 1st ed., RP-61, 1989, Recommended Practices for Evaluating Short Term Proppant Pack Conductivity.

Atteberry, R. D., Tucker, R. L., & Ritz, J. W. (1979, January 1). Application Of Sintered Bauxite Proppants To Stimulation Of Low Permeability South Texas Gas Reservoirs. Society of Petroleum Engineers. doi:10.2118/7924-MS

Auzerais, F. M. (2014, January 1). Best Practice in Hydraulic Fracturing: Reducing the Environmental Footprint. World Petroleum Congress

Boyer, J., Maley, D., & O'Neil, B. (2014, October 27). Chemically Enhanced Proppant Transport. Society of Petroleum Engineers. doi:10.2118/170640-MS

Clark, J. B. (1949, January 1). A Hydraulic Process for Increasing the Productivity of Wells. Society of Petroleum Engineers. doi:10.2118/949001-G

Cooke, C. E. (1973, September 1). Conductivity of Fracture Proppants in Multiple Layers. Society of Petroleum Engineers. doi:10.2118/4117-PA

Coulter, G. R. (1976, October 1). Hydraulic Fracturing-New Developments. Petroleum Society of Canada. doi:10.2118/76-04-03

Coulter, G.R. 1972. The Advantages of High Proppant Concentration in Fracture Stimulation, Paper SPE 3298, JPT, June 1972, Vol. 24, No. 6, pp. 643-650.

Economides, M.J. and Nolte, K.G. 2000. Reservoir Stimulation, third edition. New York: John Wiley & Sons.

Ghanizadeh, A., Clarkson, C. R., Deglint, H., Vahedian, A., Aquino, S., & Wood, J. M. (2016, August 1). Unpropped/Propped Fracture Permeability and Proppant Embedment Evaluation: A Rigorous Core-Analysis/Imaging Methodology. Unconventional Resources Technology Conference. doi:10.15530/URTEC-2016-2459818

Kong, B., Chen, S., Zhang, K., & Perdomo, M. E. G. (2015, November 9). Proppant Transport Simulation in Hydraulic Fractures and Fracture Productivity Optimization. Society of Petroleum Engineers. doi:10.2118/176873-MS

Mollanouri-Shamsi, M. M., Aminzadeh, F., & Jessen, K. (2018, April 22). Proppant Shape Effect on Dynamic Conductivity of a Fracture Filled with Proppant. Society of Petroleum Engineers. doi:10.2118/190024-MS

Novotny, E. J. (1977, January 1). Proppant Transport. Society of Petroleum Engineers. doi:10.2118/6813-MS

Palisch, T. T., Duenckel, R., Chapman, M. A., Woolfolk, S., & Vincent, M. (2010, August 1). How To Use and Misuse Proppant Crush Tests: Exposing the Top 10 Myths. Society of Petroleum Engineers. doi:10.2118/119242-PA

Palisch, T. T., Vincent, M. C., & Handren, P. J. (2008, January 1). Slickwater Fracturing: Food for Thought. Society of Petroleum Engineers. doi:10.2118/115766-MS

Schubarth, S. and Milton-Tayler, D. 2004. Investigating How Proppant Packs Change Under Stress. Paper SPE 90562 presented at the SPE Annual Technical Conference and Exhibition, Houston, 26–29 September. doi: 10.2118/90562-MS

Weaver, J. D., Nguyen, P. D., Parker, M. A., & van Batenburg, D. W. (2005, January 1). Sustaining Fracture Conductivity. Society of Petroleum Engineers. doi:10.2118/94666-MS

Zhang, J., Ouyang, L., Hill, A. D., & Zhu, D. (2014, October 27). Experimental and Numerical Studies of Reduced Fracture Conductivity due to Proppant Embedment in Shale Reservoirs. Society of Petroleum Engineers. doi:10.2118/170775-MS

APPENDIX A

SIZE DISTRIBUTION OF REMAINING PROPPANTS

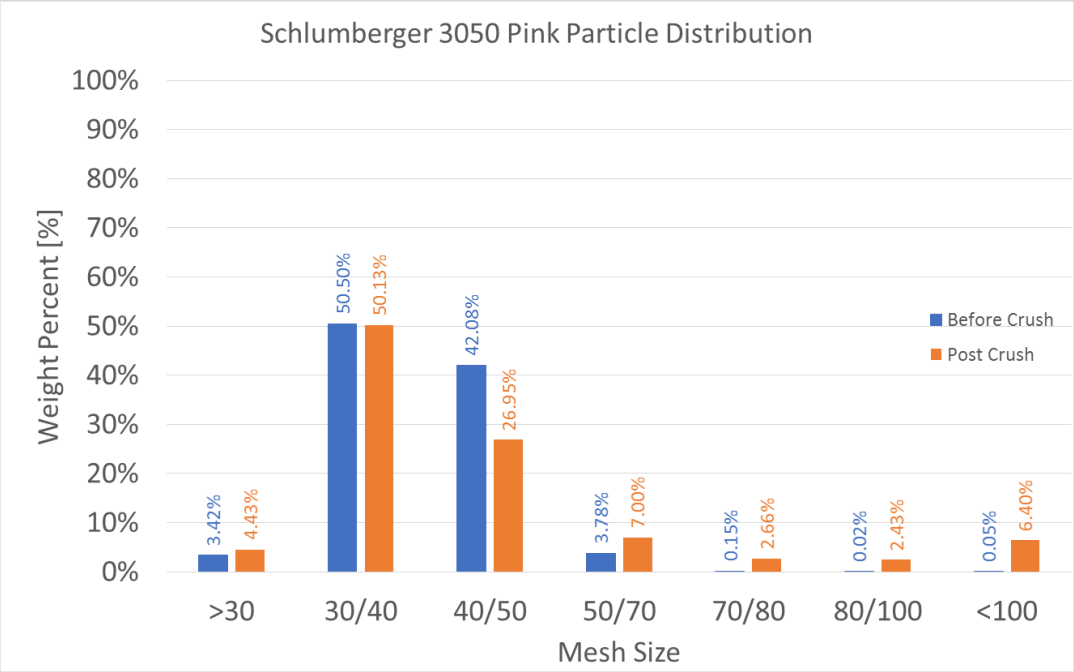

Figure A.1 Schlumberger 3050 Mesh Pink Particle Distribution

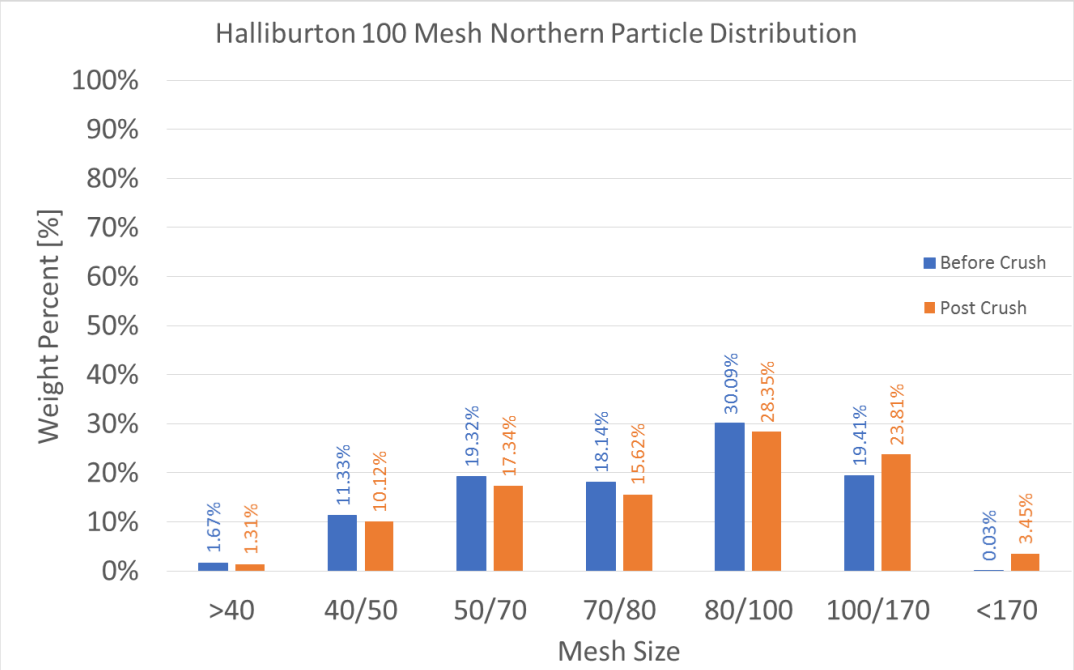

Figure A.2 Halliburton 100 Mesh Northern Particle Distribution

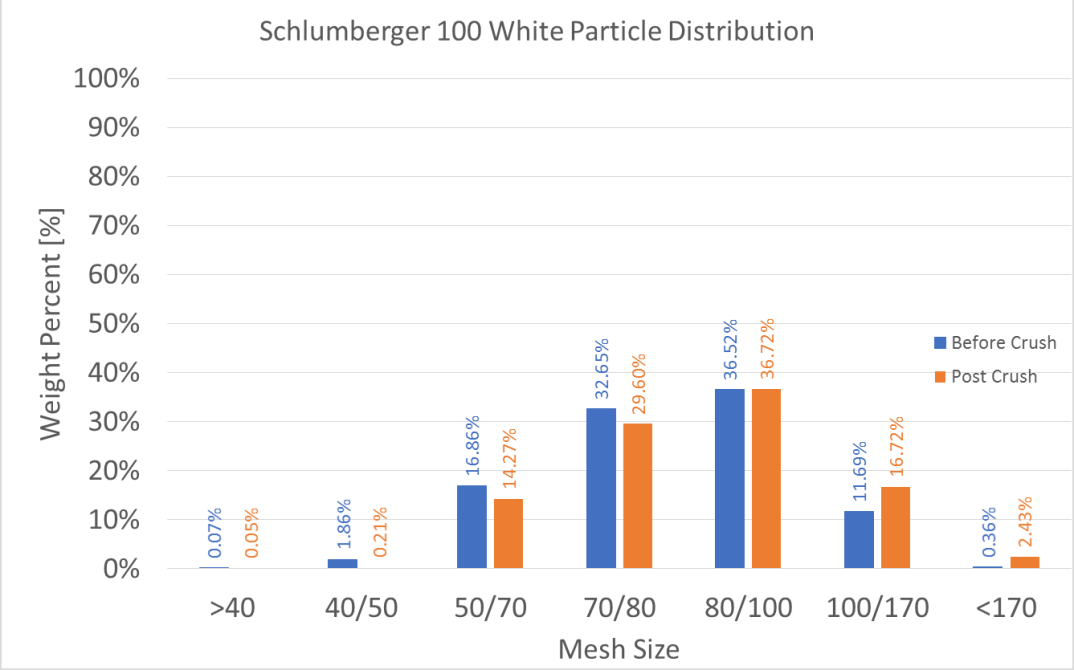

Figure A.3 Schlumberger 100 Mesh White Particle Distribution

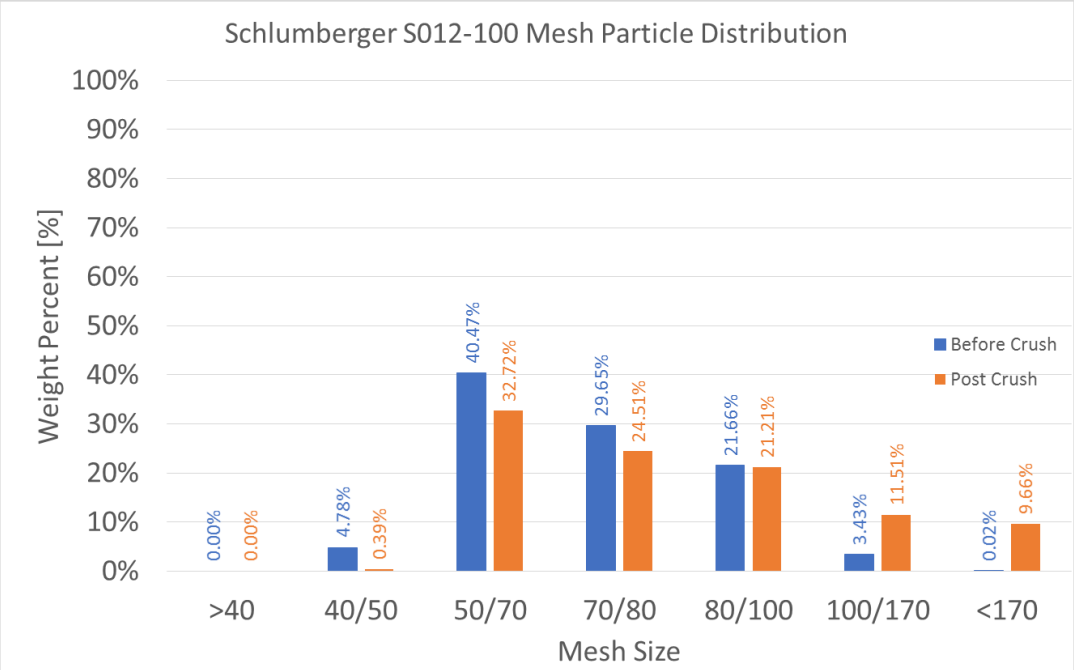

Figure A.4 Schlumberger 100 Mesh SO12 Particle Distribution

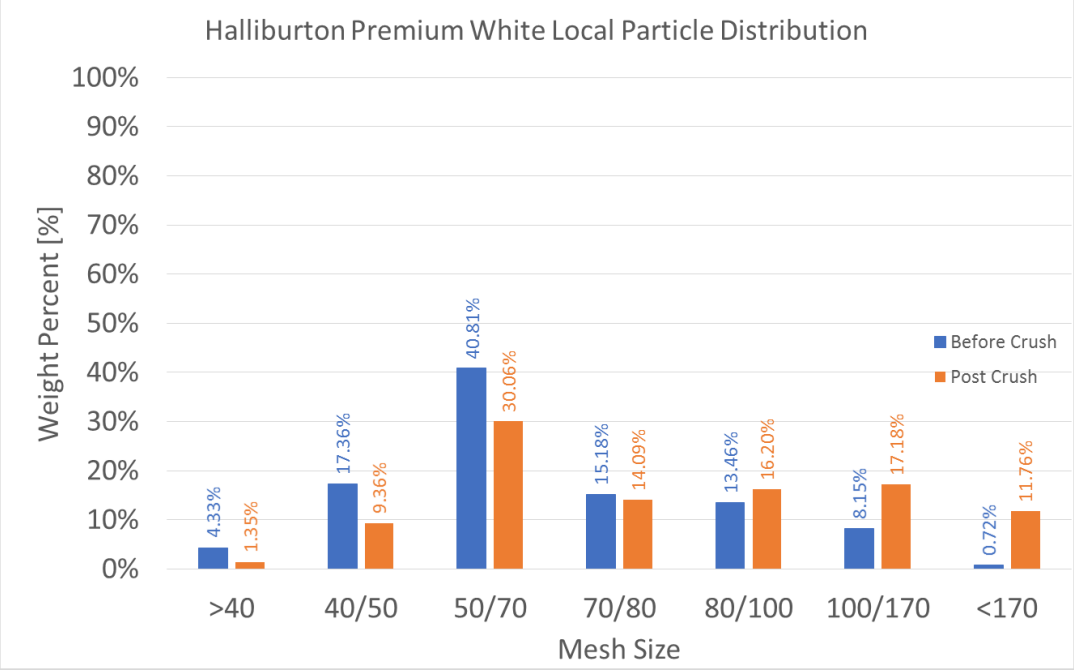

Figure A.5 Halliburton 100 Mesh Premium White Local Particle Distribution

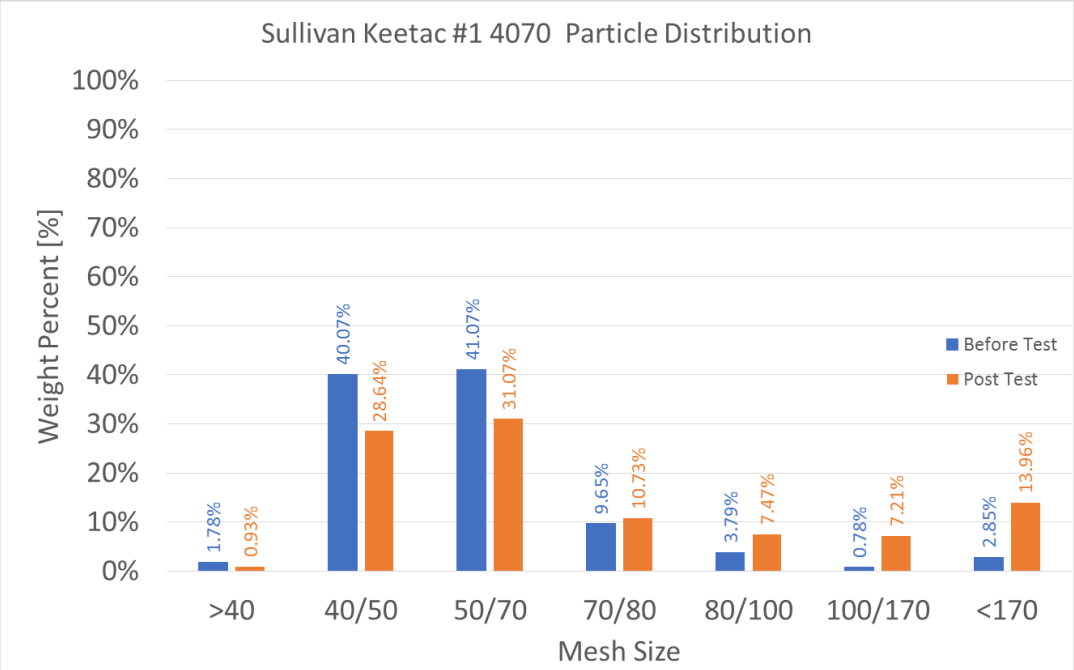

Figure A.6 Size distribution of Keetac Sample #1 4070 Mesh

APPENDIX B

4X MAGNIFICATION OF REMAINING PROPPANTS

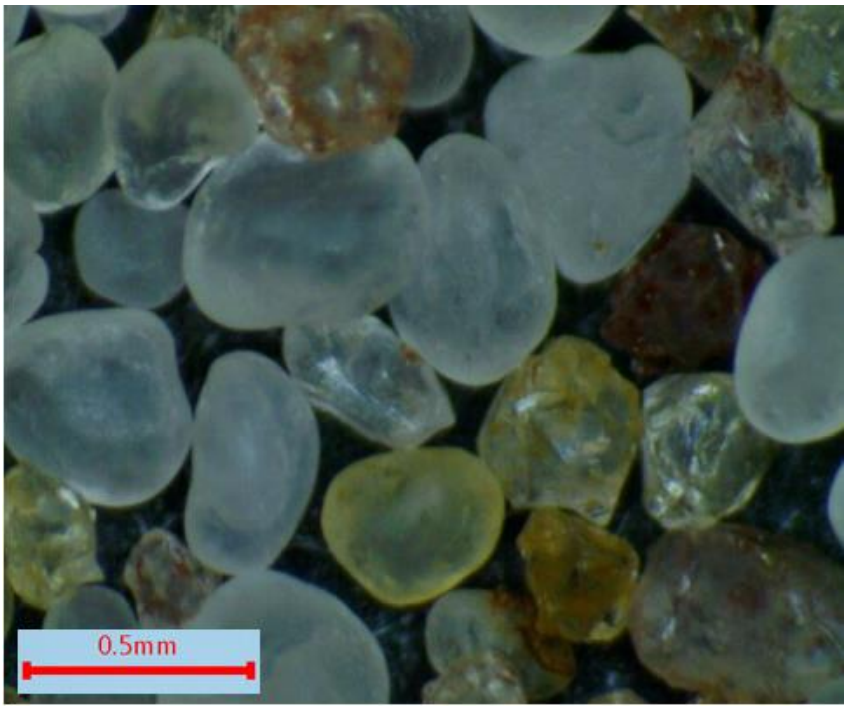

Figure B.1 Magnification of Schlumberger 30/50 Mesh Pink

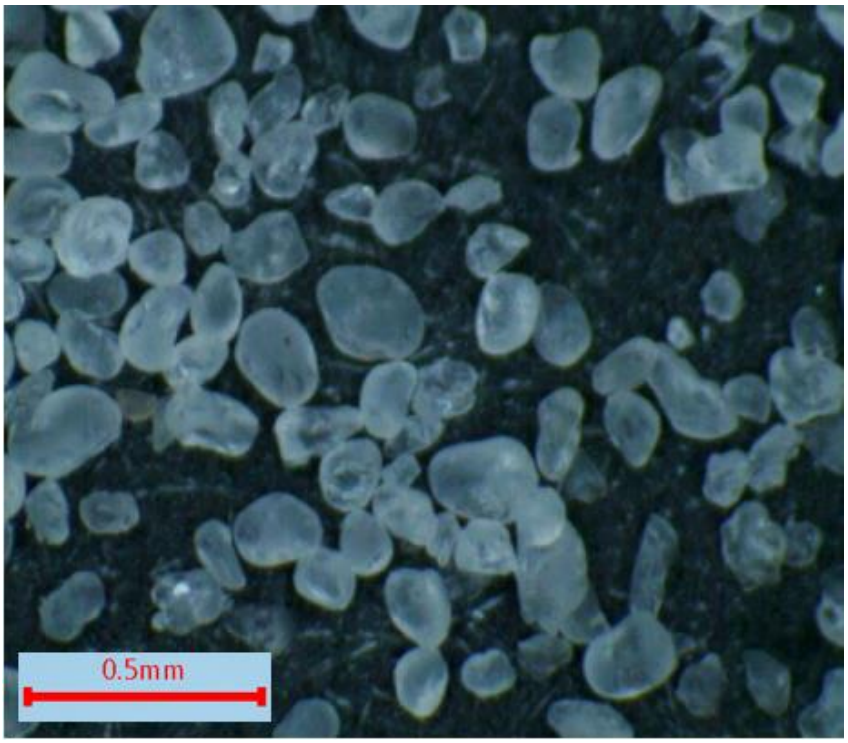

Figure B.2 Magnification of Schlumberger 100 Mesh White

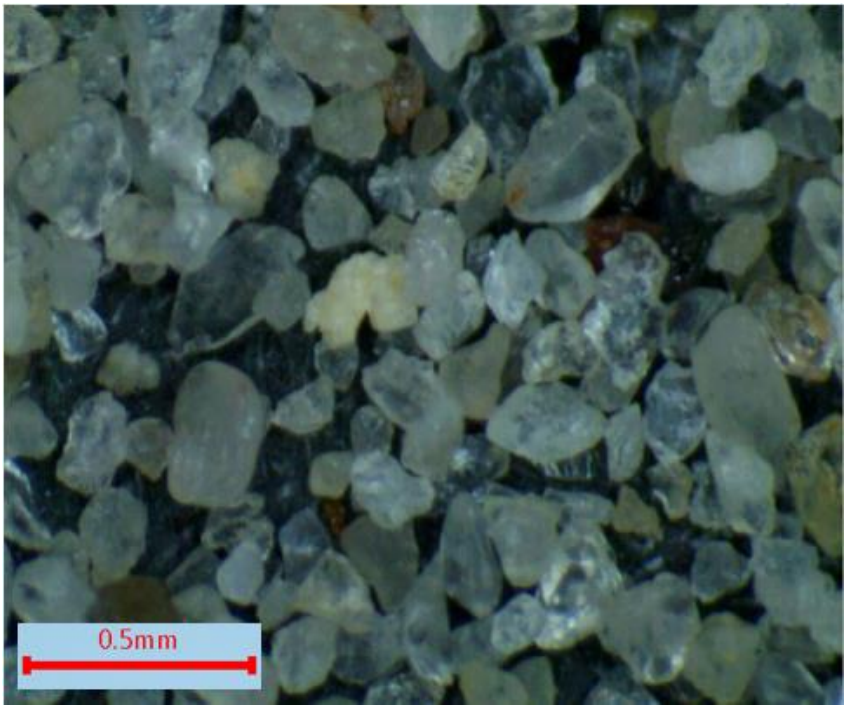

Figure B.3 Magnification of Schlumberger 100 Mesh S012 White

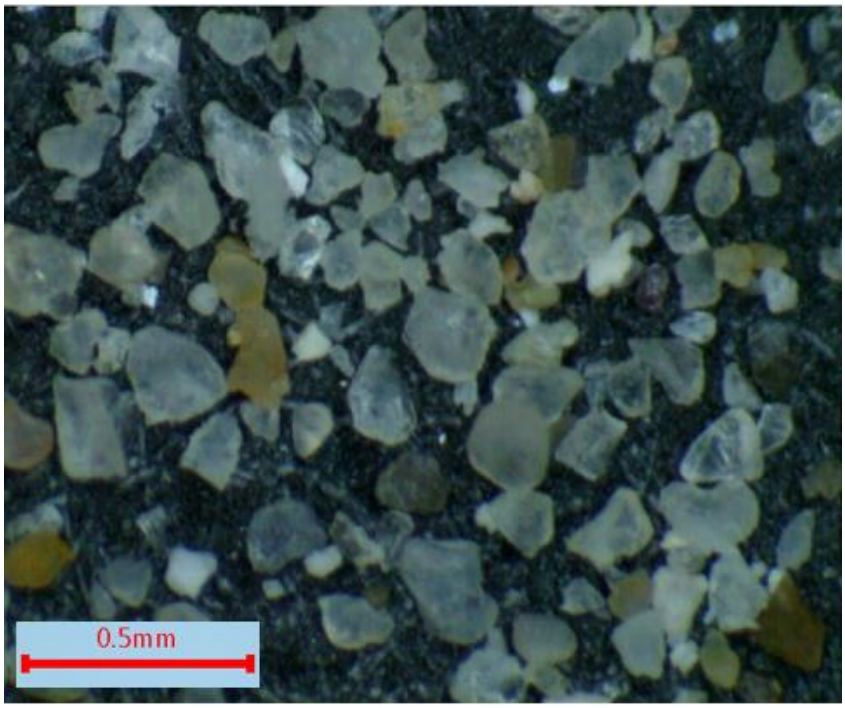

Figure B.5 Magnification of Halliburton 100 Mesh Premium White Local

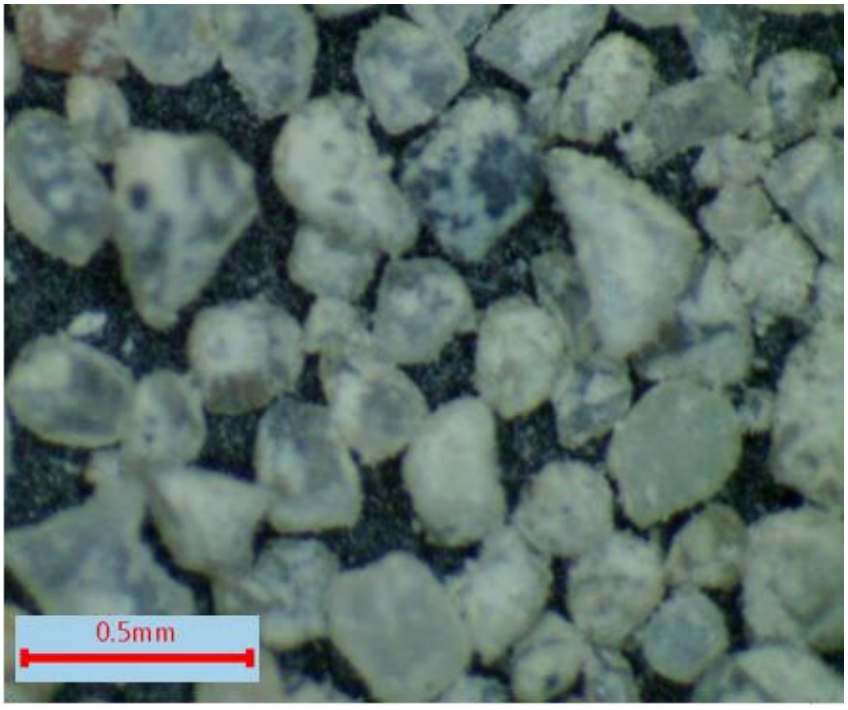

Figure B.6 Magnification of Keetac Taconite Sample #1 40/70 Mesh